Polym. Bull. (2012) 68:1425–1467
DOI 10.1007/s00289-011-0687-5

ORIGINAL PAPER

Functional polymers for photovoltaic devices

Zicheng Zuo · Yongjun Li

Received: 28 September 2011 / Revised: 12 November 2011 / Accepted: 3 December 2011 /
Published online: 13 December 2011

Abstract Solar cells based on functional copolymers were considered as promising devices and can be used to solve the intractable energy crisis for humankind. In this review, several key factors in molecular structures and morphologies which may depress the power conversion efficiency of devices are discussed first. Moreover, we concentrate on the molecular design strategies which can be applied in synthesizing functional polymers with appropriate band gap energy, prolonged exciton diffusion distance, good charge carrier transportations, as well as suitable self-assembly microphase morphologies in solid state. Once these design strategies are selectively combined, polymer solar cells with optimized performance can be approached.

Keywords Photovoltaic device · Donor–acceptor copolymer · Diblock copolymer · Double-cable copolymer · Metal-containing copolymer

Introduction

The energy crisis has become one of the most intractable problems, and new energy resources need to be explored for the growing global energy needs. The sunlight is thought to be one of the renewable and sustainable energy resources for humankind. The solar cells provide us a promising pathway to harvest the solar energy and address the emergency problem. Due to the numerous advantages, such as low cost, thin film flexibility, and ease of processing, the π-conjugated polymeric solar cells (PSC) have attracted intensive interests in both the academic and commercial

Z. Zuo · Y. Li (✉)
CAS Key Laboratory of Organic Solids, Beijing National Laboratory for Molecular Sciences (BNLMS), Institute of Chemistry, Chinese Academy of Sciences, Beijing 100190, People's Republic of China
e-mail: liyj@iccas.ac.cn

communities. Because the short lifetime excitons diffusion length is about 10 nm [1, 2], solar cells with single-component active layer and bilayer heterojunction configuration always show low power conversion efficiency (PCE) because of the poor charge carrier generation, poor transport, and limited donor–acceptor (D–A) interface [1, 3]. In recent years, the bulk heterojunction (BHJ) PSC have been intensively investigated because of the higher PCE than those of single-component active layer and bilayer heterojunction solar cells [4, 5].

In the process of light harvesting, there are four key steps taking place sequentially to convert incident solar illumination to photocurrent in PSC. In the active layer, the first step is the absorption of solar illumination, after which the photoexcitation of the donor materials produces the excitons. The number of the excitons is determined by the absorption efficiency of the polymeric molecular layers. In the second process, the photogenerated excitons need to diffuse to the D–A interface, and the diffusion length of the excitons and microphase morphologies of the films directly influence the fraction of excitons that reach the D–A interface [1, 5–7]. The increased excitons that reach the D–A interface is benefit for charge-transfer process in the third process. In the third process, the excitons arriving at the D–A interface separated into free charge through the charge-transfer process. In the last process, the fully separated electrons and holes transport to the respective electrodes under internal electric field, and then the photocurrent and photovoltage are generated. This final process is mainly determined by the morphology and mobility of the active layers. These four key steps are illuminated in Fig. 1.

The PCE of a photovoltaic device (η_{eff}) is defined as the ratio of the maximum power output to the power of the incident illumination, which is the main factor to evaluate the solar cells. The η_{eff} of the solar cell is determined by the following equation:

$$\eta_{\text{eff}} = \frac{J_{\text{sc}} V_{\text{oc}} FF}{P_{\text{in}}} = \frac{J_{\text{mpp}} V_{\text{mpp}}}{P_{\text{in}}}$$

In this equation, V_{oc} is the open-circuit voltage, J_{sc} is the short-circuit current density, FF is the fill factor of the device, and P_{in} is the incident illumination power.

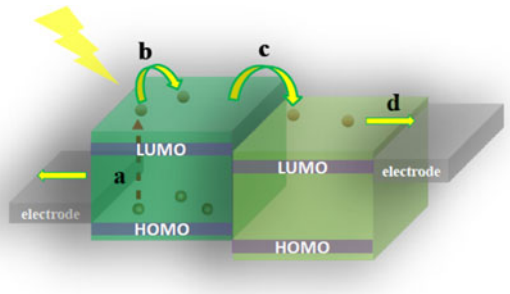

Fig. 1 The working mechanism of D–A heterojunction photovoltaic devices. (*a*) Photoexcitation of the donor to generate the excitons. (*b*) Diffusion of excitons to the D–A interface. (*c*) Exciton dissociation at the D–A microinterface resulting a geminate pair. (*d*) The charge transportation in the active layers and charge collection at electrodes

At maximum power point of the solar cell devices, the current and voltage are the J_{mpp} and V_{mpp}, respectively. It is well-known that the polymer properties play a key role in fabricating promising devices. To obtain high PCE, the functional polymers should have strong absorption efficiency overlapping with the visible light and high charge-transport properties which benefit for the charge transportation and collection in the electrodes after the charge separation and before charge recombination [6, 8]. Moreover, the suitable D–A HOMO–LUMO energy level relationships are also very important for the BHJ solar cells (Fig. 2).

Although, high efficiency can be obtained in conventional polymeric photovoltaic devices, the disordered and non-uniform phase structures of thin film are still the main factors to compromise the device efficiency (Fig. 3a). The compromised efficiency is due to the short exciton diffusion length in the active layers and the limited charge collection in the electrodes. To address these problems in devices, several conventional methods can be adopted such as annealing [9, 10], spin-coating speed [11, 12], and solvent treatment [13–16] and so on. The ideal phase structure of the film (Figs. 3b, 4, 5, 6, 7, 8, 9, 10, 11, 12, 13, 14, 15, 16, 17, 18, 19, 20, 21, 22, 23, 24, 25, 26, 27, 28) is considered to be composed of dense patterned array of nanostructure with dimension in exciton diffusion length. In the ideal structure, the D–A phase structure will have straight pathway to the electrodes, which will minimize the charge-transfer distance and charge recombination, and every exciton formed will be in the exciton diffusion length [5, 17]. More and more investigations

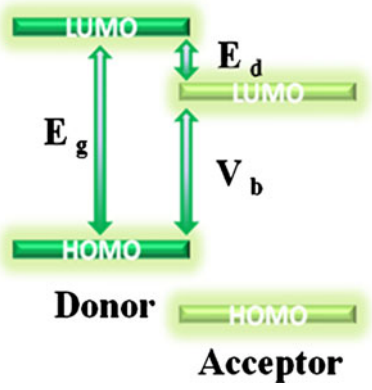

Fig. 2 Energy diagram of donor and acceptor HOMO–LUMO levels in the PSC. E_g is the band gap of the donor polymers, E_d is the LUMO energy difference serving as a driving force for electron transfer, and V_b is the built-in potential showing a linear relationship with the open-circuit voltage (V_{oc})

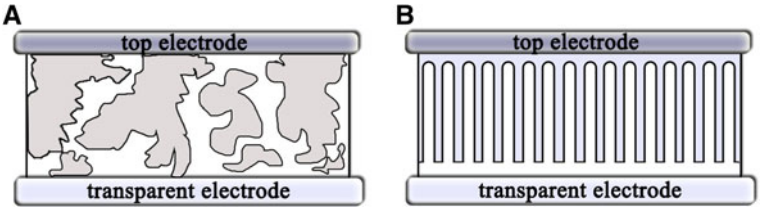

Fig. 3 The disordered BHJ solar cell (**a**) and the solar cell with ideal structure (**b**)

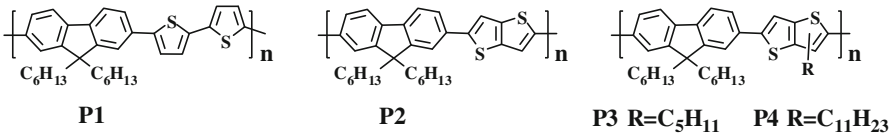

Fig. 4 Chemical structures of **P1–P4** containing fluorene and thiophenes

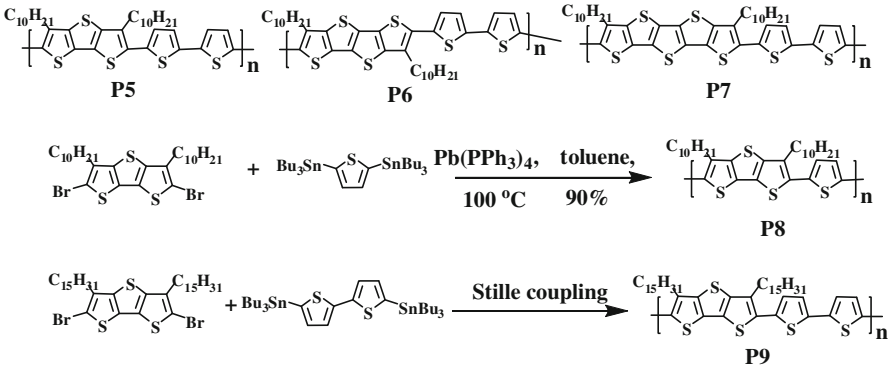

Fig. 5 Alternating copolymer structures of **P5–P9** containing fused thiophenes

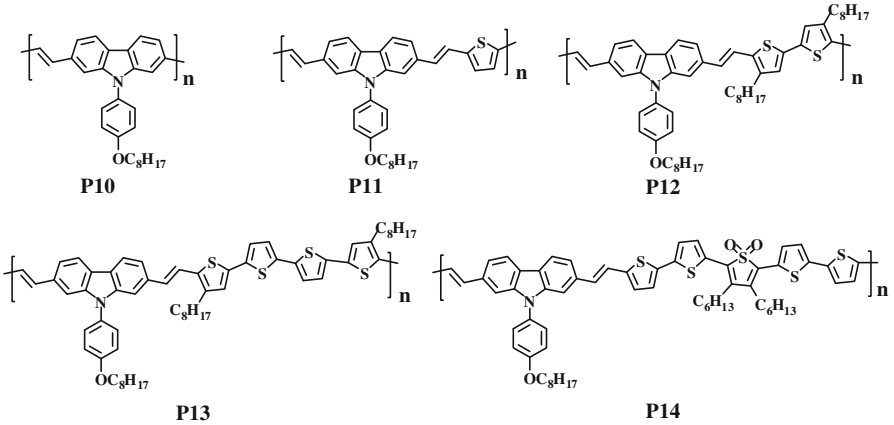

Fig. 6 Five poly(2,7-carbazole)-based copolymers with diverse lengths of oligothiophenes

have adopted this ideal structure to improve device efficiency, including dye-sensitized solar cells and PSC [18–20].

From the above working mechanism, the PCE equation and the microphase structures in the PSC, it is concluded that there are several key factors to be solved for construction of efficient PSC, such as the absorption efficiency of donor materials, the charge-transport properties, the morphologies of the active layer, and the acceptor properties. For construction of an ideal PSC, the p-type conjugated

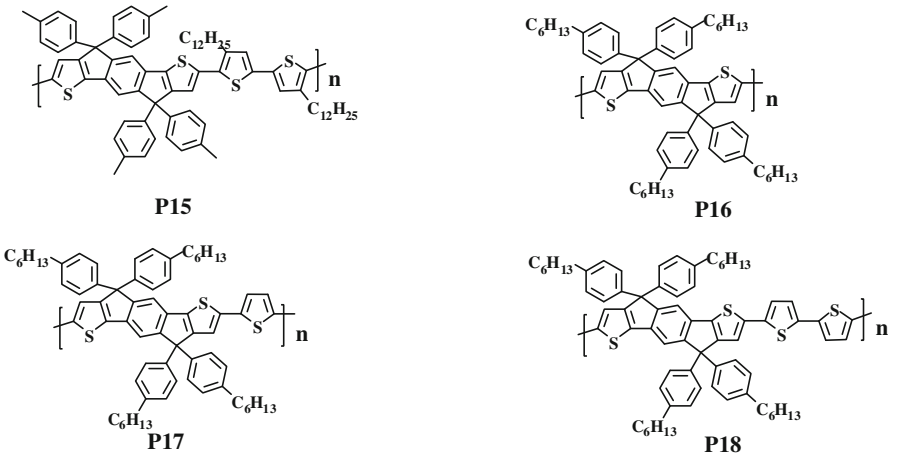

Fig. 7 Four conjugated copolymers based on coplanar TPT derivatives

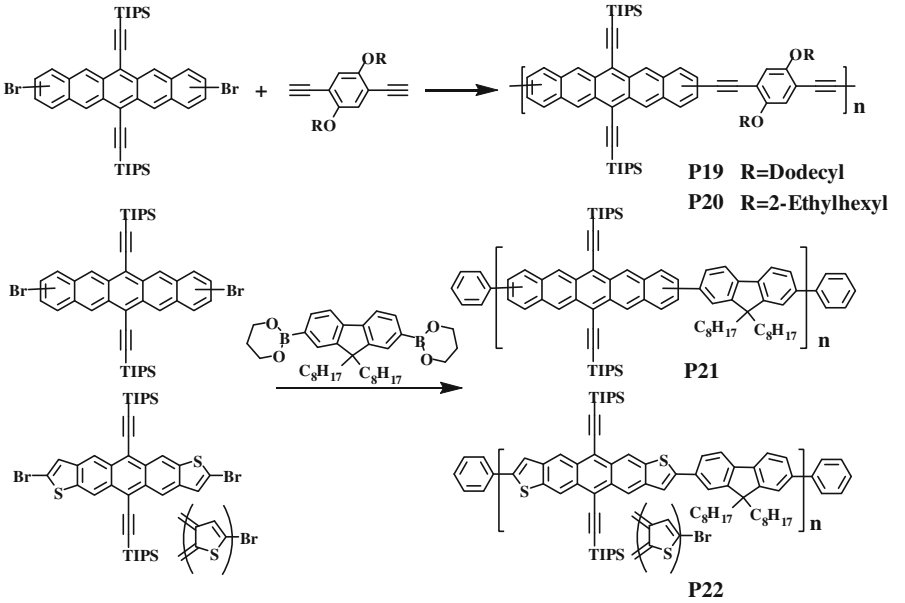

Fig. 8 Synthesis of copolymers **P19–P22** containing acenes and heteroacenes

polymers should simultaneously possess good film-forming properties, good absorption efficiency, high charge carrier mobility, as well as suitable HOMO–LUMO energy levels and good microphase morphologies. Deeply understanding the molecular design principle and the benefits of versatile polymer synthesis allow for the effective tailoring of the intrinsic properties of conjugated polymers to serve the desired purpose and address the application needs.

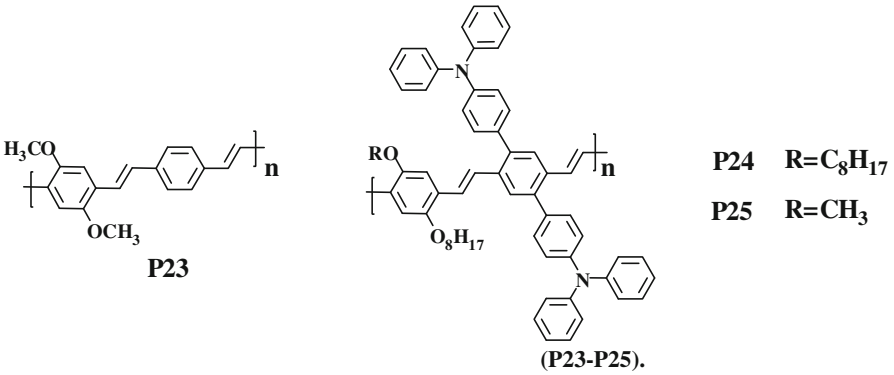

Fig. 9 PPV derivatives with electron-donating group (**P23**–**P25**)

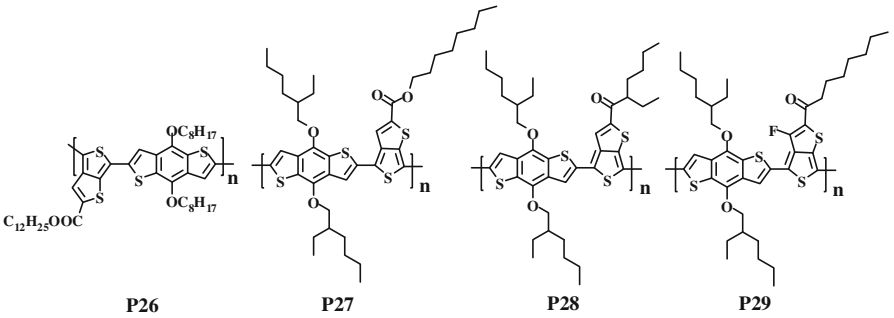

Fig. 10 Copolymers based on BDT and bithiophenes for OPV applications (**P26**–**P29**)

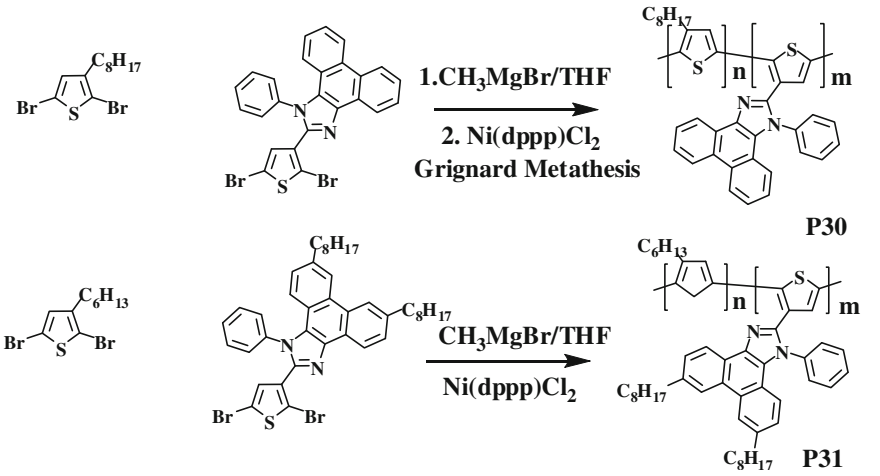

Fig. 11 Polythiophene derivatives containing electron-withdrawing groups (**P30**–**P31**)

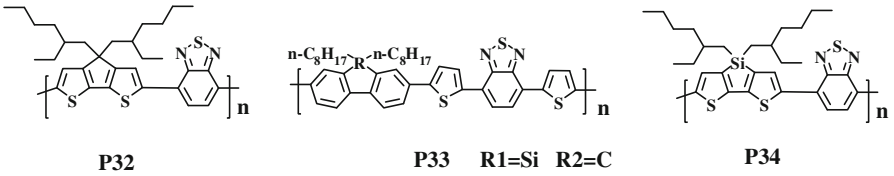

Fig. 12 Structures of D–A alternating copolymers containing silicon atom

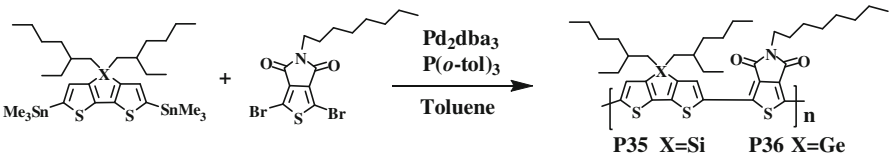

Fig. 13 Synthesis of D–A copolymers containing silicon **P35** and germanium atom **P36**

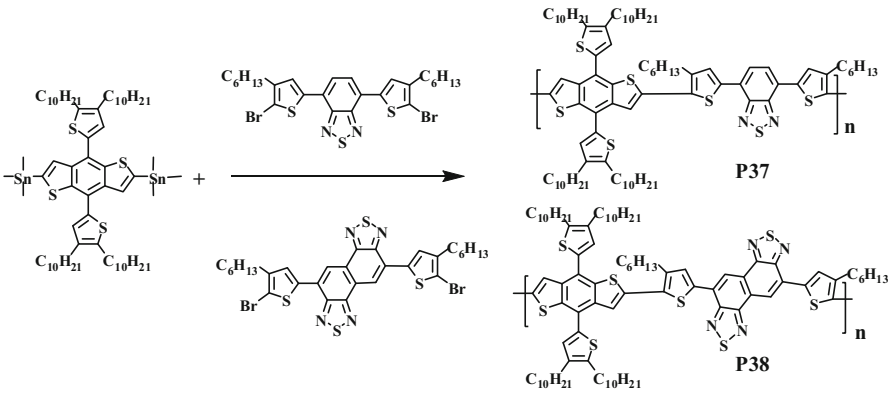

Fig. 14 The synthesis of copolymer **P37** and **P38**

In this review, we will mainly concentrate on the molecular design strategies which can be applied in synthesizing functional polymers with appropriate optical properties, prolonged exciton diffusion distance, suitable self-assembly properties in solid state and so on. These strategies provide us valuable pathways to optimize the efficiency of polymeric photovoltaic devices.

Copolymers composed of donor moieties

Due to the versatility in structure modification and great electronic tunability, many polymers have been served as sensors [21–26] as well as solar cell materials during this decade. By the development of conjugated copolymers such as poly(phenylethene) (PPE) [27], poly(*p*-phenylenevinylene) (PPV) [28–32] and polythiophenes,

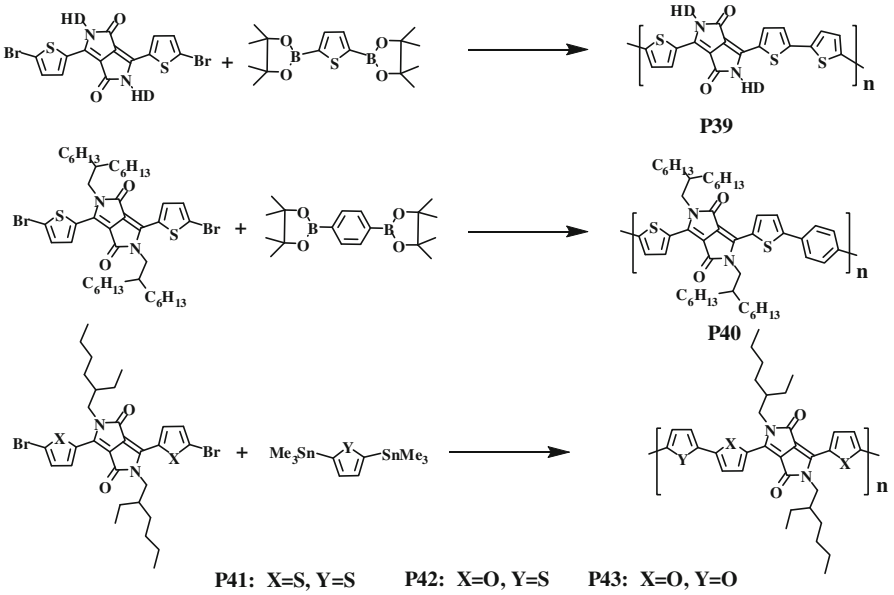

Fig. 15 The synthesis of copolymers based on diketopyrrolopyrrole moiety (**P39–P43**)

Fig. 16 Chemical structure of copolymers **P44–P47**

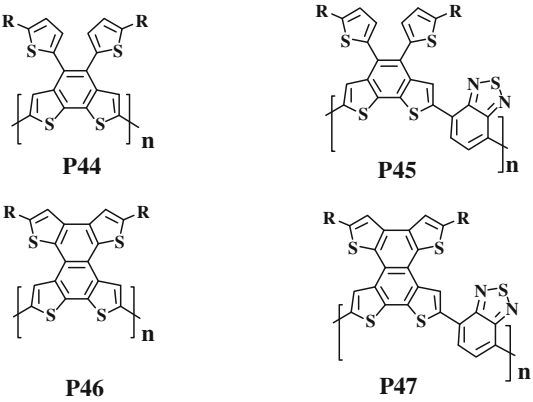

more and more copolymers composed of donor moieties were synthesized and investigated, and showed promising properties in flexible PSC. By introduction of some suitable donor moieties, the band gap of copolymers can be straightforwardly reduced by raising the HOMO energy level, therefore, the broader absorption property may be resulted in. During the process of designing small band gap polymers through this method, the overall absorption coefficients of copolymers are also important and should not be sacrificed [33]. In this section, the copolymers composed of various electron-rich segments along the main chain will be discussed.

Fluorene unit is a promising electron-rich building block due to the deep-lying HOMO energy levels and good hole-transporting property which are crucial

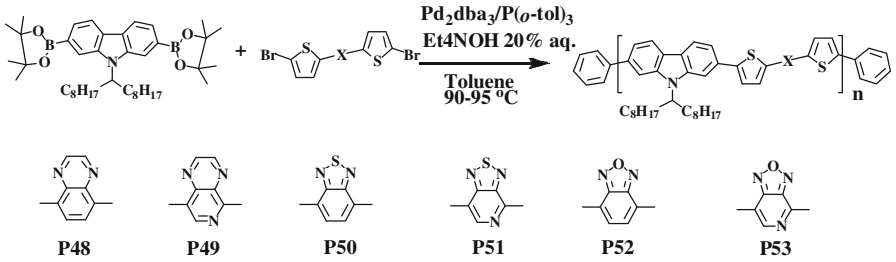

Fig. 17 D–A copolymers containing diverse acceptor groups (**P48**–**P53**)

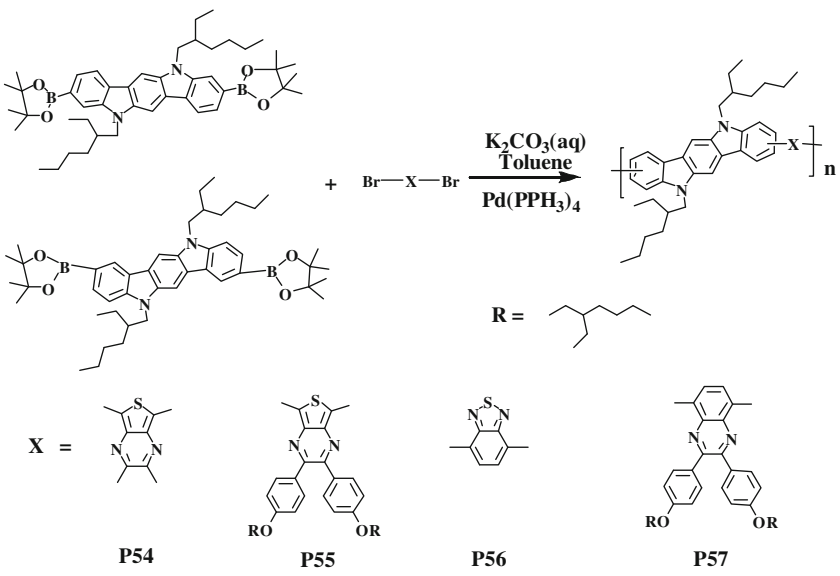

Fig. 18 The synthesis of D–A copolymers based on indolo[3,2-b]carbazole group

prerequisites to achieve high V_{oc} [34]. Polymers containing fluorene derivatives have attracted considerably attention in the optoelectronic area due to their excellent hole-transportation, easy modification and stability properties [35, 36]. Conjugated polymer **P1** containing alternating fluorene and electron-rich bithiophene units was prepared [37] in Holdcroft's group. The HOMO and LUMO levels of **P1** were estimated to be −5.41 and −2.52 eV, respectively. The extended conjugation along the backbone reduced the optical band gap to 2.41 eV. The photovoltaic device based on **P1**:PCBM (1:4, w/w) blend film absorbed light between 300 and 500 nm, and a high V_{oc} of 1.03 V and a moderate PCE value of 2.7% were obtained due to the high hole mobility and well-defined nanophase segregation morphology. Compared to **P1**, Chen and co-workers [38] obtained alternating conjugated copolymers (**P2**–**P4**) comprised of fluorene and thieno[3,2-b]thiophene moieties using the Suzuki coupling reaction. The polymers exhibited good thermal stability with decomposition temperature in the region of 308–431 °C. Photovoltaic cells

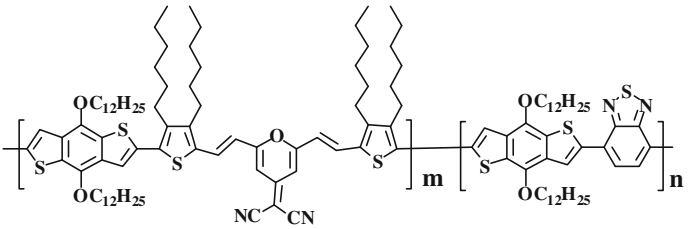

Fig. 19 D–A copolymers containing two kinds of acceptor moieties (**P58**)

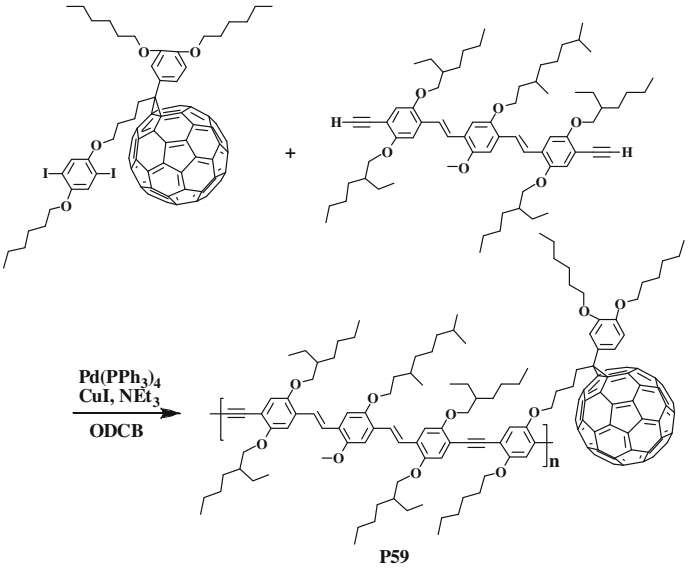

Fig. 20 The synthesis of double-cable copolymer using Sonogashira method

Fig. 21 The double-cable copolymer containing perylenediimide group

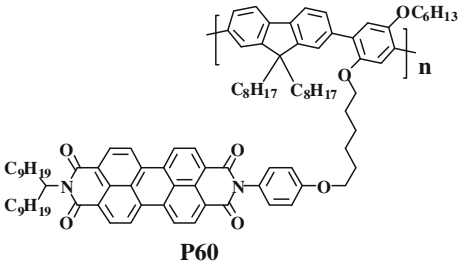

properties based on these polymers with the configuration of ITO/PEDOT-PSS/polymer: PCBM (1:1, w/w)/Ca/Ag were investigated, respectively. The incident photon to converted electron current efficiency of the device was found to be about 2%, and the low PCE might be partially due to the poor fill factor and narrow

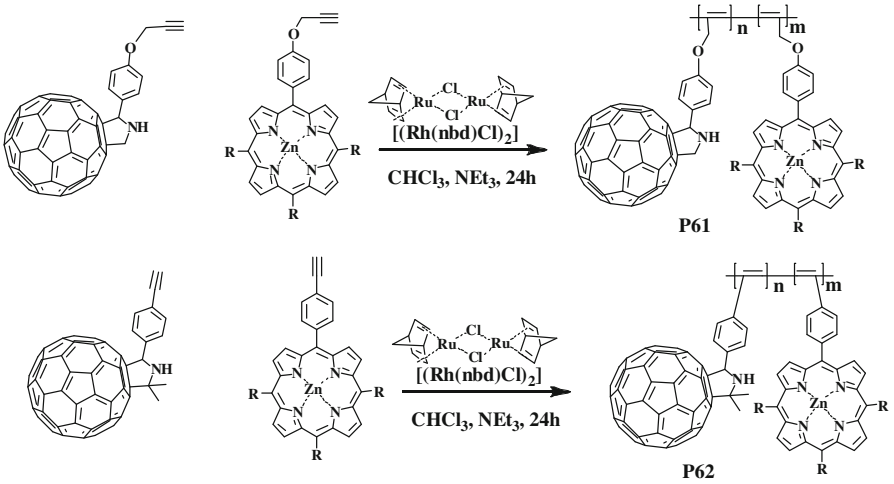

Fig. 22 The synthesis of copolymers (**P61**, **P62**) composed of fullerenes and porphyrins

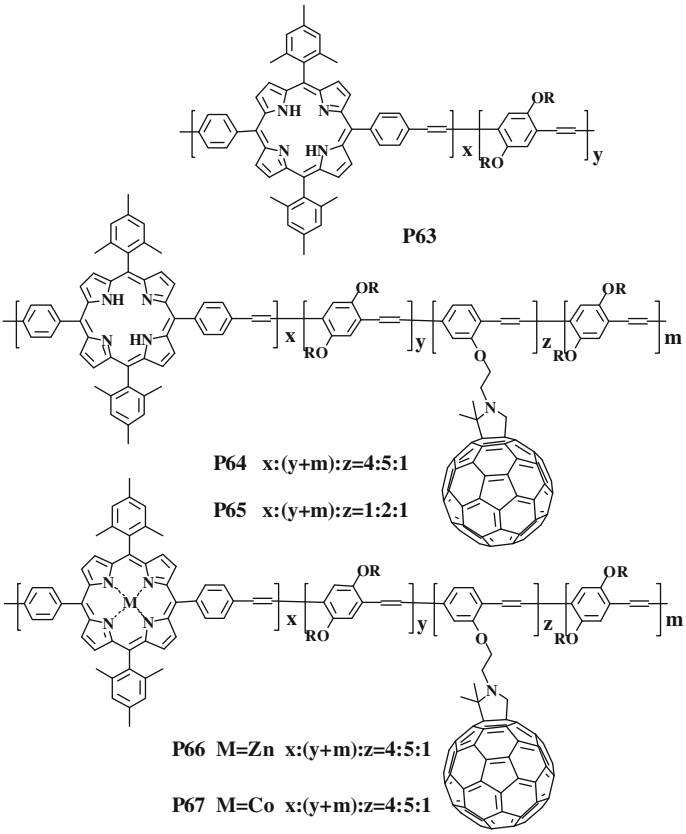

Fig. 23 The chemical structures of copolymers (**P63**–**P67**)

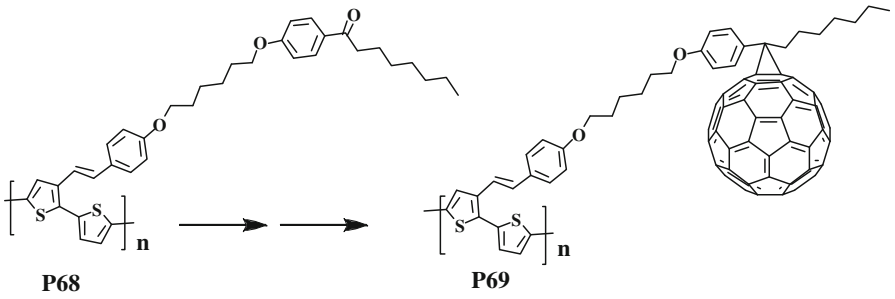

Fig. 24 The synthesis of double-cable copolymer **P69** based on polythiophene and fullerene

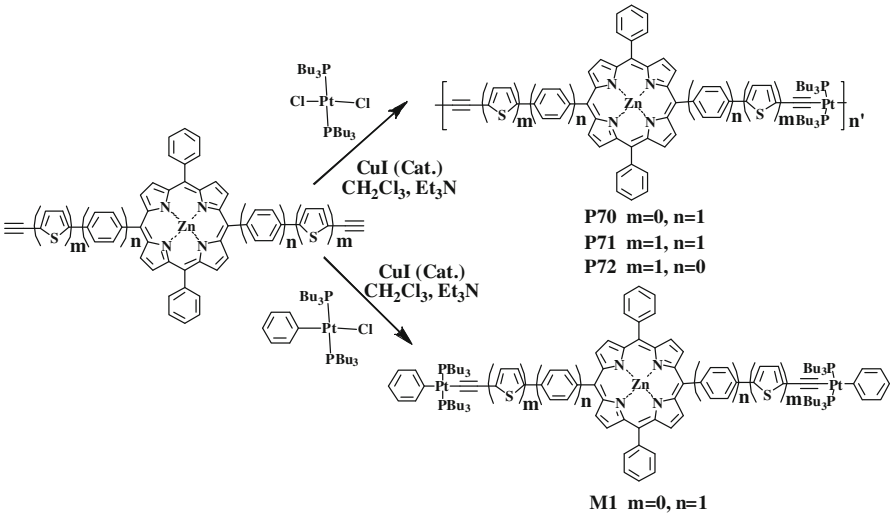

Fig. 25 The synthesis of copolymer **P70–P72**

absorption in the range of 300–500 nm for the polymers. Moreover, the light-emitting diodes based on **P1–P4** were investigated, and **P1** and **P2** exhibited pure green emission with more excellent spectral stability and robust emission than **P3** and **P4**.

Derivatives of fused thiophene ring have been well investigated during the past years and showed good charge carrier mobility in OFET [39]. Due to the outstanding electronic properties and coplanar structures with extended π systems, the fused thiophene rings were introduced into the copolymer backbones, and devices based on **P5–P7** were prepared with high-mobility in He et al. [40]. The excellent charge carrier mobility derived from the extended π systems and well-organized solid structures are also helpful for the fabrication of photovoltaic devices with high efficiency. Zhan and co-workers [41] prepared copolymer **P8** containing dithieno[3,2-b:20,30-d]-thiophene (DTT) structure using Stille coupling reaction.

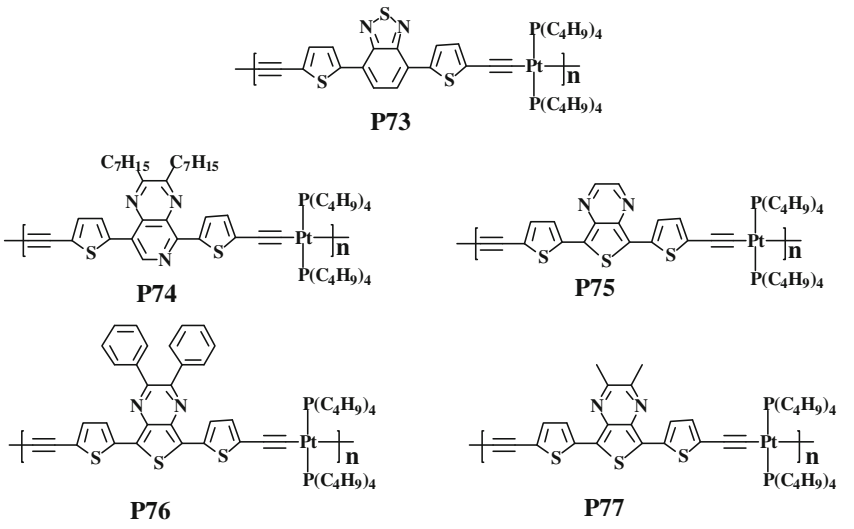

Fig. 26 The chemical structures of copolymer **P73–P77**

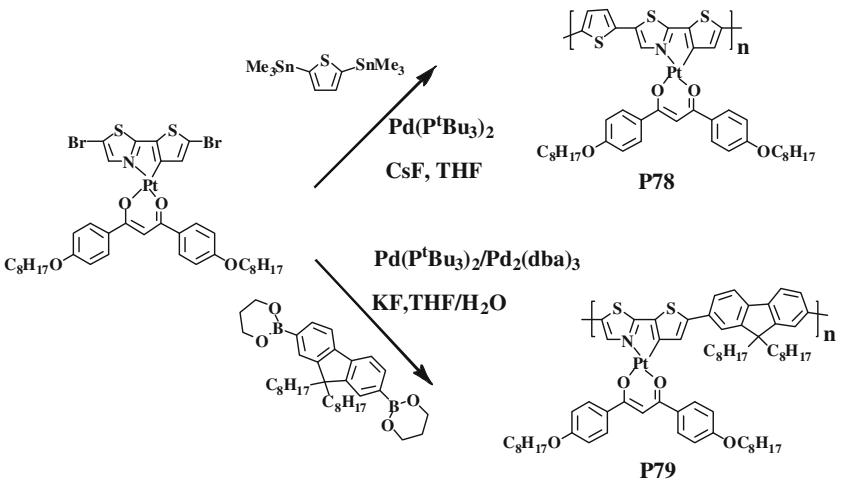

Fig. 27 The synthesis of copolymer **P78** and **P79**

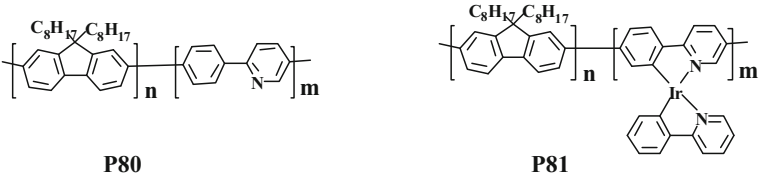

Fig. 28 Copolymer structure of **P80** and **P81**

From cyclic voltammetry, the HOMO and LUMO energies of the polymer **P8** were estimated to be −5.4 and −3.4 eV, respectively. The polymer showed a strong absorption peaked at 518 nm in thin film with an optical band gap 2.0 eV. BHJ solar cells with structure of ITO/PEDOT:PSS/polymer:PCBM/Al were fabricated based on the blend of the polymer **P8** and $PC_{61}BM$ with diverse weight ratio. The highest PCE of 0.37% was achieved under AM 1.5, 100 mW/cm ^{2} using **P8**:PCBM (1:4, w/w) as active layer, and the PCE was optimized to 0.7% after thermal treatment. Different with Zhan's research, Ong and co-workers [42] introduced longer alkyl side chains to the β-positions of DTT unit, and copolymerized DTT with 5,5′-bis(trimethylstannyl)-2,20-bithiophene. The copolymer **P9** had a relatively high molecular weight as well as good solubility. The solution-processed FET device exhibited a mobility of 0.06 $cm^2/(V\ s)$ and a current on/off ratio more than 10^6, which were much better than those earlier reported for analogous polymers. More importantly, the performance of BHJ photovoltaic devices based on **P9** and $PC_{71}BM$ was quite remarkablely improved, and the PCE was over 3%, which showed competitive efficiency compared with some best polymer semiconductors. This result indicated that the DTT was an efficient unit for copolymers used in OTFT and OPV applications.

Similar to fluorene, 2,7-carbazol is also an electron-rich moieties, and can be incorporated into the conjugated copolymers. As a donor materials, poly(2,7-carbazole)-based copolymers play promising role in photovoltaic devices [34, 43]. Leclerc and co-workers [44] synthesized several copolymers containing 2,7-carbazole in the backbone (**P10–P14**), and investigated their properties in photovoltaic devices. By incorporating with diverse length of oligothiophenes, the optical and electronic properties of copolymers were well tuned. As the length of oligothiophenes increased in the backbone (**P10–P13**), the absorption band was red-shifted and the optical band gaps were decreased from 2.3 to 2.0 eV. However, the addition of *S*,*S*-dioxide thiophene moiety in **P14** induced a more significant bathochromic shift and the band gap was greatly reduced to 1.7 eV due to the intramolecular D–A interaction. BHJ photovoltaic cells with structure feature of ITO/PEDOT/polymer:PCBM (1:4, w/w)/Al from different copolymers **P10–P14** and $PC_{61}BM$ had been fabricated without optimization treatment, and the PCEs of these devices were about 0.4, 0.4, 0.3, 0.2, and 0.8%, respectively.

For polymer-based photovoltaic devices, effective light harvesting and high carrier mobility properties are both key issues in improving the PCE. The introduction of fused ring is considered to increase the rigidity of the molecular backbone and conjugation degree, and can also benefit to decrease chain folding, which may limit the charge carrier mobility at higher molecular weights [45]. Ko and co-workers [46] investigated conjugated polymers based on the coplanar thiophene–phenylene–thiophene (TPT) derivatives. The UV–Vis absorption spectra indicated that the optical band gaps of **P15–P18** were about 2.1 eV, and compared to regioregular P3HT, **P17** and **P18** both had higher absorption coefficient. The thin film field-effect carrier mobilities of the coplanar semiconducting polymers were investigated based on bottom-contact geometry. An improved field-effect hole mobility of 3.0×10^{-3} $cm^2/(V\ s)$ and on/off ratios (1.3×10^6) can be obtained from **P18** FETs processed from the higher boiling dichlorobenzene solutions.

Furthermore, FETs prepared from the other copolymers (**P15**–**P17**) showed similar or relatively lower performances compared with **P18** FETs. Except for the fabrication of FETs with good performance, the BHJ solar cells were constructed with the structure feature of glass/ITO/PEDOT:PSS/polymer:PCBM/Ca/Al, and the solar cell were fabricated based on the blend of polymers and $PC_{61}BM$ or $PC_{71}BM$ with the weight ratio of 1:3. The maximum PCE of the devices based on **P17**/PC_{71}BM system reached 3.3% with a short-circuit current density of 7.6 mA/cm^2, an open-circuit voltage of 0.8 V, and a fill factor of 0.54 under AM 1.5G (100 mW/cm^2) illumination. The results indicate that the copolymers containing coplanar TPT derivatives are promising solar cell materials.

Fused acenes and heteroacenes such as pentacene, anthradithiophene, and their derivatives showed relatively low band gap, and have been extensively investigated for organic field-effect transistors [47], and due to the extended π-conjugated system, these materials show promising charge-transfer properties in solid states. By incorporating these fused units into backbones, conjugated copolymers with low band gaps and good charge-transfer properties may be produced. In addition, the large fused rings may potentially increase the intermolecular π–π stacking in the solid state for efficient charge transport. Bao and co-workers [48, 49] synthesized several conjugated copolymers containing fused acene and heteroacenes using Sonogashira coupling and Suzuki cross-coupling polymerization. From CV, the HOMOs and LUMOs were calculated to be 5.28 and 3.57 eV for **P19** and 5.24 and 3.54 eV for **P20**, respectively and the band gaps of **P19** and **P20** were about 1.69 and 1.70 eV, respectively. Compared to pentacene, the increased stabilities and low band gaps were due to the incorporation of pentacene into the conjugated polymer backbone, which led to high delocalization of π-electrons on pentacene ring and making it less electron rich. Incorporating with fluorenes, **P21** and **P22** also showed red-shifted absorption spectra compared with their monomers and had optical band gaps of 1.78 and 1.98 eV, respectively. BHJ solar cells were fabricated using polymer **P22**:PCBM (1:3, w/w) blend as the active layer, giving a J_{sc} of 2.35 mA/cm^2, a V_{oc} of 0.75 V as well as a PCE value of 0.68%.

Due to the good optoelectronic properties and easy modification of the chemical structures, poly(*p*-phenylenevinylene)s have attracted more and more attention during the past decade, and can be served as the important photovoltaic materials. It is well-known that triphenylamine (TPA) moiety and its derivatives are 3D propeller groups and good hole-injecting/transporting materials. The introduction of TPAs to functional copolymers will tune the optoelectronic properties and the charge carrier mobility of the solid films by changing the intramolecular π-electron distribution in the backbone. Li and co-workers [50] designed three different PPV derivatives (**P23**–**P25**). In **P24** and **P25**, two TPA groups were attached directly as the two side groups of phenylenevinylene backbones, and the 3D intermolecular π–π stacking structures were prepared which was different from **P23** structure. The HOMO and LUMO energy levels estimated from cyclic voltammogram were about 5.05 and 3.00 eV for **P24**, and 5.0 and 2.89 for **P25**, respectively. Comparing with **P23**, the introduction of TPA side chains in **P24** and **P25** along these backbones greatly increased the HOMO energy level of **P24** and **P25**, respectively, and lowered the optical band gap to 2.25 and 2.0 eV, respectively. Therefore, the

resulting copolymers exhibited strengthened and broadened absorption spectra in the visible region. The BHJ photovoltaic cells based on **P24** or **P25** and PCBM (1:1, w/w) showed PCE up to 0.27 and 0.45% under the illumination of AM 1.5, 90 mW/cm^2, which were about three to five times higher than that of the device based on **P23** (0.09%) without TPA side chains. The greatly improved PCE of the devices from **P24** and **P25** could be attributed to broader absorption region and enhanced hole-transporting properties of these copolymers.

After the synthesis of benzo[1,2-b;3,4-b]dithiophene (BDT) unit, its derivatives were widely introduced into functional copolymers for field-effect transistor devices and devices with high hole mobility were obtained [51, 52]. The promising performance of these kinds of copolymers has attracted intensive attention in the field of photovoltaic devices. BDT is a completely symmetric moiety and regioregular conjugated copolymers can be easily synthesized by the introduction of BDT, which can enhance the intermolecular order in the solid state. In addition to this good property, BDT is an excellent electron-rich group and can be added to reduce the optical band gap. Yu and co-workers [53] developed the copolymer **P26** based on the BDT group that really attracted greatly interest. **P26** was synthesized via the Stille coupling reaction between an ester substituted 2,5-dibromothieno[3,4-b]thiophene and dialkoxyl benzodithiophene distannane comonomer. With the introduction of thieno[3,4-b]thiophene groups, the quinoidal structure of the backbone will be stabilized and the energy gap of the copolymers will be narrowed [54]. The HOMO and LUMO were determined to be −4.90 and −3.20 eV from cyclic voltammetry, respectively, and the optical band gap energy calculated from the onset of the film absorption was about 1.62 eV. Without special optimization treatments, the simple BHJ solar cells with structure feature of ITO/PEDOT:PSS/polymer:PCBM/Ca/Al exhibited a high solar energy conversion efficiency of 5.6%, high fill factor of over 65% as well as V_{oc} of 0.58.

Hou and co-workers [55] further optimized the copolymer structures by modification of the thieno[3,4-b]thiophene group. Comparing to **P26**, **P27** substituted the long dodecyl group with octyl group, and the small change decreased the HOMO energy to −5.01 eV and increased the V_{oc} to 0.62 V. However, lower PCE of 5.15% than that of **P26** was obtained because of the lower fill factor. Previous researches indicated that the alkyloxy chain had a much stronger electron-donating effect than an alkyl chain, and increased the HOMO energy level of poly(3-alkoxythiophene) [56]. In **P28**, the alkyloxy group was substituted with an alkyl side chain, and lower HOMO and LUMO energy levels than that of **P27** were observed from **P28** than that of **P27**. Different with **P28**, the fluorine atom was introduced to the thieno[3,4-b]thiophene unit in **P29**, and the HOMO and LUMO levels were further lowered to −5.22 and −3.45 eV, respectively. The PCE of the solar cells based on **P28**/PCBM blends showed impressive result, up to 6.58%. At the same time, the device based on **P29**/PCBM blends achieved the best PCE of 7.7%. Compared with **P26** and **P27**, the optimized PCEs from polymer **P28** and **P29** were both derived from the increased V_{oc} (0.7 and 0.76 V, respectively), J_{sc} (14.7 and 15.2 mA/cm^2, respectively), and fill factor (64.1 and 66.9%, respectively) in the devices.

D–A alternating copolymers

Except for introducing the electron-rich groups into the backbone to tune the optical band gap, incorporating both the donor and acceptor groups directly into conjugated copolymer backbone is also considered to be an effective pathway for perturbing the molecular orbitals through either inductive or mesomeric effects, and has been widely used in designing low band gap conjugated copolymers for solar cells [57]. Normally, in D–A copolymers, the electron-rich moieties raise the HOMO energy, while electron-deficient moieties lower the LUMO energy, resulting in a controllable band gap. In the D–A copolymers, the donor and acceptor segments exhibit electron pushing and pulling properties, respectively [58]. Therefore, the introduction of push–pull driving forces along the conjugated backbones can facilitate electron delocalization and the formation of quinoid structures ($D–A \rightarrow D^+ = A^-$) over the conjugated backbone [33]. Compared to the aromatic form, the quinoid form is energetically less stable and smaller band gap. The population of quinoid form will be increased when the aromaticity of the aromatic units in the backbone was reduced. Therefore, the D–A copolymers with controllable band gap can be prepared by introduction of electron-rich and electron-deficient groups in the backbone.

Numerous studies indicated that polythiophene derivatives were one kind of the most important materials for photovoltaic devices due to their excellent light absorption and electron conductivity [59, 60]. To further improve the PCEs of this kind of BHJ polymer solar cells, Wei and co-workers [61, 62] used Grignard metathesis polymerization to synthesize a regioregular polythiophene derivative with side chain of phenanthrenylimidazole groups, in which polythiophene and phenanthrenylimidazole separately served as the donor and acceptors. By controlling the number of phenanthrenyl-imidazole moieties in the copolymers, the optical band gap energies of **P30** were successfully tuned from 1.89 to 1.77 eV. Relative to those of pure polythiophene, the lowered band gap and fast charge transfer in **P30** both contribute to much higher external quantum efficiencies (EQEs) and higher J_{sc}. In particular, the device J_{sc} based on copolymer containing 80% phenanthrenylimidazole, was improved from 8.7 to 14.2 mA/cm^2 for the device of pure poly(3-octylthiophene). In addition, the maximum PCE was increased to 2.80% for **P30** from 1.22% for poly(3-octylthiophene). To further improve the solubility of this kind of polymers, two octyl chains were used to modify the phenanthrenylimidazole. The J_{sc} of devices fabricated from a copolymer **P31** with 90 mol% octylphenanthrenyl-imidazole moieties was optimized to 13.7 mA/cm^2 compared with the 8.3 mA/cm^2 observed from poly(3-hexylthiophene) devices and the maximum PCE based on this particular copolymer was up to 3.45%. The increased PCE based on **P30** and **P31** suggested that such kind of copolymers with acceptor side groups were promising polymeric photovoltaic materials.

2,1,3-Benzothiadiazole was widely introduced into conjugated polymers with D–A alternating structures. Mühlbacher et al. [63] prepared the novel low-band gap copolymer **P32** containing 2,1,3-benzothiadiazole and cyclopentadithiophene units. The structure offered not only good charge-transport properties and fitting electronic energy levels but also good processability. The cyclic voltammetry indicated that

P32 showed an electrochemical band gap of 1.73 eV in solution, while the optical absorption data suggested a lower optical band gap of 1.6 eV in solid state films. From the solar cell devices based on **P32**/$PC_{71}BM$ blends, PCE of 3.2% and J_{sc} of 10–11 mA/cm^2 were obtained with the fill factor of 47%. Based on **P32**, further investigations were carried out by Heeger and co-workers [64]. A few volume percent of alkanedithiols were introduced into **P32**/$PC_{71}BM$ solution as co-solvent before preparing the films. Interestingly, the PCEs of photovoltaic cells were increased from 2.8 to 5.5% by the introduction of alkanedithiols. Further investigations indicated that alkanedithiols played an important role in tuning the BHJ morphologies in the active layer without further treatment [65]. This discovery provided an efficient method to control microphase structures easily where thermal annealing and other treatments were either undesirable or ineffective.

Cao and co-workers [66] used silicon atom to substitute the carbon atoms on the 9-position of the fluorene and prepared copolymer **P33**. By the introduction of silicon atoms, BHJ photovoltaic devices with higher V_{oc} (0.90 V), J_{sc} (9.5 mA/cm^2), and fill factor of 50.7% were achieved, while the FET devices showed increased hole mobility (1×10^{-3} cm^2/(V s)). Therefore, compared to the devices based on copolymer without substitution, the PCE of **P33** increased up to 5.4%. Combining the superiority of both **P32** and **P33**, Yang and co-workers [67] synthesized a low-band gap copolymer **P34**. The FETs of **P34** demonstrated that the hole mobility was greatly enhanced to 3×10^{-3} cm^2/(V s), which is about three times higher than that for Si-substituted **P33**. Photovoltaic properties of this material were investigated without further optimization, and a PCE of up to 5.1% was obtained under AM 1.5G, 100 mW/cm^2 illumination, and the response range of the device covered the whole visible range from 380 to 800 nm. Further investigation of quantum mechanical calculations and grazing incidence, X-ray diffraction suggested that silicon atom substituted moiety enhanced the solid-state ordering compared to the carbon-fused analogue (**P32**), leading to efficiently improved charge transport, due to a stronger intermolecular π-stacking interaction [68].

Yang and co-workers [67, 69] synthesized copolymer **P34** with promising properties in photovoltaic devices. This result indicated that the D–A alternating copolymers containing electron-rich segments of fused-ring heterocycles might also exhibit good PCE, and this strategy could greatly increase the copolymer species for solar cells. Based on Yang's research, Reynolds and co-workers [70] obtained D–A alternating copolymers consisting fused-ring heterocycles donor with silicon (**P35**) and germanium atom (**P36**) and they thought that the substitution of the bridging carbon or silicon atoms for the larger germanium atom might further enhance the intermolecular ordering, because the long C–Ge bond lengths would further remove the bulky side chains from the planar heterocycle and strengthen the intermolecular π-stacking. The MM2 optimized geometry indicated that the methyl groups were further displaced from the conjugated backbone in Ge-bridged heterocycles than in Si-bridged heterocycles, therefore the larger surface was benefit for π–π stacking. The intensive π–π stacking was considered to be helpful for obtaining high hole mobility, which could result in improved PCE of photovoltaic devices. BHJ solar cells were fabricated using **P35** and **P36**:$PC_{71}BM$ blends as active layers with inverted device architectures ITO/ZnO/Polymer: PC70BM/MoO_3/Ag. From

illuminated (A.M 1.5) *J–V* curves of both **P35** and **P36**, it was shown that with 5% 1,8-diiodooctane (DIO) as a processing additive the performance of both polymers was greatly enhanced, and both the J_{sc} and FF were significantly increased. After optimization, solar cell based on **P35** achieved an average PCE of 6.6% with J_{sc} of 11.5 mA/cm 2, V_{oc} of 0.89 V, and FF of 65%, and device of **P36** obtained PCE of 7.3% with J_{sc} of 12.6 mA/cm^2, V_{oc} of 0.85 V, and FF of 68%. The EQE spectra of the devices were also carried out and demonstrated that without DIO devices displayed fairly low quantum efficiency across the visible region. The increased EQE provided the possibility to achieve high PCE. Further investigations of atomic force microscopy (AFM) and transmission electron microscopy (TEM) proved that the addition of processing additive strongly influenced the device morphologies and resulted in uniform phase separation. Recently, the device PCE based on **P35**/$PC_{71}BM$ have been optimized up to 7.3% in Chu et al.'s [71] study.

In Cao and Huang's investigation [72], the electron-deficient unit, naphtho[1,2-c:5,6-c]bis[1,2,5] thiadiazole (NT), which consists of two fused 1,2,5-thiadiazole rings, have been synthesized and introduced into the conjugated copolymer **P38**. Compared with the copolymer **P37** consisting of single 1,2,5-thiadiazole rings, copolymer **P38** exhibited lower optical band gap due to the stronger electron-withdrawing capability. The fused two 1,2,5-thiadiazole rings increased the planar aromatic structure, which would benefit the interchain stacking of the resulting copolymer and may further enhance the hole mobility. From absorption spectra, the NT-based copolymer **P38** exhibited a red-shifted absorbance and the optical band gap of **P38** was decreased from 1.73 eV for **P37** to 1.58 eV, which was considered to be much closer to the ideal band gap for PSC donor materials [73]. The space charge limited current model was used to measure the mobilities of both **P37** and **P38**, and the result indicated that **P38** had a much higher hole mobility than **P37**. Therefore, the lower band gap and high hole mobility together increased the PCE of solar cell, and the PCE of 5.32 and 6.00% were obtained from **P38**/PC61BM and **P38**/PC71BM with weight ratio of 1:1, which was obviously higher than 1.56% (**P37**/PC61BM) and 2.11% (**P37**/PC71BM).

Strongly absorbing diketopyrrolopyrrole (DPP) moieties were considered as efficient electron-deficient moieties and have been widely introduced to lower the band gap in functional small molecules and copolymers. The DPP moiety exhibited a planar-conjugated bicyclic structure, which leads to strong π–π interactions. The small D–A molecules containing DPP were applied in fabricating solar cells, and showed excellent properties with PCE up to 4% in BHJ solar cells [74–76]. DPP-containing copolymers were considered to be promising materials and showed attractive properties in thin-film transistors with very high hole mobilities on the order of 1 cm^2/(V s) [77]. Therefore, intensive studies were carried out to investigate the photovoltaic applications of DPP-containing copolymers [78, 79]. In the study of Janssen and co-workers [78, 79, 81, 82], a series of copolymers containing DPP were prepared, and these copolymers all showed promising properties in solar cells. Typical copolymers **P39** and **P40** were both synthesized by Suzuki cross-coupling method [78, 79]. From the cyclic voltammetry, the HOMO and LUMO levels of **P39** were found at −5.17 and −3.61 eV, respectively. The optical band gap energy was about 1.36 eV in *o*-dichlorobenzene solution and

1.30 eV in thin films. The FET fabricated from **P39** exhibited nearly balanced hole and electron mobilities of 0.04 and 0.01 $cm^2/(V\ s)$, which may be optimal factor for photovoltaic devices. Photovoltaic devices based on **P39**/PC61BM were fabricated with DIO as the cosolvent, and the best device gave V_{oc} of 0.68 V, a fill factor of 0.67, a J_{sc} of 8.3 mA/cm^2, and the PCE was about 3.8%. When the solar cells were prepared using **P39**/$PC_{71}BM$ mixture with optimal weight ratio (1:2), it provided V_{oc} of 0.65 V, J_{sc} of 11.8 mA/cm^2, and FF of 0.60, resulting in an improved PCE of 4.7% due to the increased photocurrent in the visible region.

Polymerizing with benzenediboronic ester, the **P40** were synthesized and the energy levels of **P40** were determined by cyclic voltammetry with a HOMO at −5.35 eV and LUMO at −3.53 eV. FETs were fabricated in a bottom-gate bottom-contact geometry and exhibited ambipolar behavior with electrons and holes mobilities of 0.02 ± 0.01 and 0.04 ± 0.01 $cm^2/(V\ s)$, respectively. Photovoltaic cells were fabricated by spin coating **P40** and PCBM solution with optimized weight ratio (1:2) onto ITO/PEDOT:PSS electrode and evaporation of LiF/Al as a back contact. By the addition of a cosolvent DIO, morphology of the thin films can greatly be improved and affording a much finer phase separation, thereby the PCE of the solar cell were remarkably enhanced from 2% with the acceptor of $PC_{61}BM$ and $PC_{71}BM$ to 4.6% ($PC_{61}BM$) and 5.5% ($PC_{71}BM$).

In the study of Fréchet and co-workers [80], the furan moiety was introduced into the DPP-containing copolymers and the properties in solar cell of these copolymers were investigated. Compared to copolymer **P39**, the furan moiety can be conjugated into backbones without reducing their solar cell performance, and can greatly improve the solubility of copolymers. The onset of absorption spectra of the copolymer thin films indicated that the optical band gaps were 1.41 eV for **P42** and 1.35 eV for **P43**. From the cyclic voltammetry, the HOMO and LUMO energy levels of were determined about −5.4 and −3.8 eV for **P42**, and −5.5 and −3.8 eV for **P43**, respectively. These properties were comparable to those obtained from low band gap copolymer **P41**. Solar cells involving **P42**/PCBM active layers were prepared with the device structure ITO/PEDOT:PSS/polymer:PCBM/LiF/Al. Meanwhile, a small amount of 1-chloronaphthalene was used as the additive to prepare thin film with optimal morphology. When $PC_{61}BM$ served as the acceptor, solar cells with PCE of 3.7% were prepared. While $PC_{71}BM$ was used to increase the breadth of the photoactive spectrum and the overall photocurrent, the average PCE was improved to 4.7%. The best device achieved a V_{oc} of 0.74 V, a J_{sc} of 11.2 mA cm^{-2}, a fill factor of 60%, and a PCE of 5.0%. Solar cells based on **P43**/$PC_{71}BM$ active layers were also fabricated and achieved an average PCE of 3.8% (max 4.1%) after optimization.

Not only the optical band gap but also the assembly morphologies of copolymers are necessary to obtain good photovoltaic efficiency. Introduction of monomers with extended π-conjugated systems provide an efficient way to tune both the band gap and assembly structures. In the study of You and co-workers [83], the electron-rich unit benzo[2,1-b:3,4-b′]dithiophene were brought into the functional polymers, and oxidative photocyclization process were carried out to expand the coplanar structures. Compared to **P45**, the hole mobility of **P47** were obviously increased from 4.21×10^{-6} to 1.3×10^{-5} $cm^2/(V\ s)$. Therefore, the improved mobility of

P47, helped achieve much higher short-circuit current than those of related solar cells with open-ring unit based polymers. Without photocyclization, the devices PCEs based on **P44** and **P45** were about 0.1 and 0.6%, respectively. However, after photocyclization, the devices PCEs based on **P46** and **P47** were significantly improved to 2.03 and 2.06%, respectively. The morphology of these devices was characterized with AFM, scanning electron microscopy and TEM in order to estimate the microphase separation. Compared to **P46**/PCBM film, the **P47**/PCBM film exhibited less refined microstructure with grain sizes in hundreds of nanometers, however, with very homogenous microstructures in each of these grains. Therefore, the additional explanation for the low hole mobility and relatively low current of **P47**/PCBM devices can be obtained from the characterization of film morphology. Recently, some new D–A copolymers have been prepared and showed excellent efficiency up to 7% in the study of You and co-workers [84, 85].

The design and introduction of various electron-withdrawing groups play a great role in tuning the LUMO of copolymers. Leclerc and co-workers synthesized a series poly(2,7-carbazole) derivatives with tunable acceptor segments (**P48**–**P53**) [86] using Suzuki coupling reaction. Theoretical calculations and experiments both revealed that HOMO energy level of these copolymers was mainly determined by the carbazole moiety, whereas the LUMO energy level was mainly related to the nature of the electron-withdrawing units. From **P48** to **P53**, the LUMO energy level were tuned to −4.32, −3.67, −3.60, −3.80, −3.65, and −3.93 eV, respectively, and the optical band gaps of thin films were 2.02, 1.89, 1.88, 1.75, 1.87, and 1.67 eV, respectively. Photovoltaic devices based on polymer/PCBM blends were characterized and the results indicated that the most efficient polymers were those with a symmetric structure. The highest device PCEs based on **P50** and **P52** were 2.4 and 3.6%, respectively, which were due to the high hole carrier mobility and well-organized morphologies of symmetric structures. Further optimization treatment has been carried out for **P50** solar cell by Bazan and co-workers [87]. By incorporating an ultrathin-conjugated polyelectrolyte (CPE) layer of poly[3-(6-trimethylammoniumhexyl)thiophene] or poly(9,9-bis(2-ethylhexyl)-fluorene]-*b*-poly[3-(6-trimethylammoniumhexyl)thiophene] between the active layer and the metal cathode, the PCE of solar cells based on **P50**/$PC_{71}BM$ blends can be increased from 5 to 6.5%. The investigation indicated that the deposition of the CPE layer induced the increase of V_{oc} and J_{sc}, which optimized the PCE of solar cell. The device fabrication provided a considerably simple, promising and practical method to prepare polymer solar cells with high efficiencies and did not need thermal annealing.

The indolo[3,2-b]carbazole has expanded π-conjugated structures and can be regarded as two carbazole fused together. It has been proved that this group shows strong electron-donating ability. Moreover, indolo[3,2-b]carbazole and indolo[3,2-b]carbazole containing polymers showed good stability and field-effect transistor mobility [88, 89]. Chen and co-workers [90] introduced indolo[3,2-b]carbazole moiety into the D–A alternating copolymers, and combining with different acceptors, and a series of D–A copolymers were synthesized (**P54**–**P57**). The optical band gap of this kind of copolymers were well tuned from 1.58 to 2.34 eV. The photovoltaic cells PCE of the indolocarbazole-based copolymer/PC_{61} BM or

PC_{71} BM were in the range of 0.14–1.40% under the illumination of AM 1.5G (100 mW/cm^2). In these studies, **P57** exhibited the best PCE performance among these copolymers due to its suitable band gap, high molecular weight, good hole mobility, efficient photoluminescence quenching, and large V_{oc}.

Normally, D–A copolymers containing one fixed donor and acceptors have been intensively investigated during past years. However, D–A copolymers containing two different acceptors are freshly studied. Tian and co-workers [91] synthesized a series of copolymers combining benzo[1,2-b:4,5-b0]dithiophene donor and two acceptors with different ratios. The electrochemical characterizations showed that by increasing the benzothiadiazole ratio the HOMO energy level were gradually increased from −5.43 to −5.12 eV with nearly fixed LUMO levels. The optical results indicated that the optical band gap of the copolymers were effectively tuned from 1.70 to 1.84 eV. The BHJ solar cells were fabricated by using the blends of copolymers and PCBM as the active layer. The photovoltaic characters revealed that the V_{oc} was gradually increased from 0.7 to 0.94 V when the HOMO energy levels of copolymers were decreased, meanwhile, three optimized factors of increased absorption spectrum in the visible region, optimized hole mobility and microphase morphologies of blend films greatly optimized the J_{sc}. With a V_{oc} of 0.78 V, J_{sc} of 5.47 mA/cm^2, fill factor of 0.40, the PCE of photovoltaic cell based on copolymer **P58** ($m = n$) was optimized to 1.67% under simulated AM 1.5 solar irradiation of 100 mW/cm^2. This was due to the high hole mobility and interpenetrating network morphology of **P58**:PC_{61} BM blend active layer. The photovoltaic device based on **P58**:PC $_{71}$ BM showed a even higher J_{sc} of 8.32 mA/cm^2 and a higher PCE up to 2.89%. Incorporating with more electron-rich and electron-deficient groups is a powerful method to prepare novel copolymers, however, the symmetry of copolymers will be greatly reduced and the molecular stacking will be greatly influenced. Therefore, the charge-transfer property of the solid films will also be influenced.

Double-cable copolymer

Double-cable polymers provides an efficient way to achieve semiconducting materials with both p-type (hole conducting) and n-type (electron conducting) properties[92], moreover, the covalent structure can produce a homogeneous phase morphologies of the donor/acceptor domains, and the interface between the donor and acceptor can be maximized. During the past decade, there were increasing interests in the preparation of active electronic materials combining both p-type and n-type moieties.

The palladium-catalyzed Sonogashira and Suzuki cross-coupling methods can be performed under mild conditions, which provide us efficient methods to prepare double-cable copolymers. Numerous fullerene [93–101] and perylenedimiides [102–107] derivatives were synthesized during the past decades and this greatly increased the category of double-cable copolymer. Janssen and co-workers [108, 109] had synthesized and investigated a series of copolymers with pendant fullerenes and perylenediimides. **P59** contained both double and triple bonds in the

backbone, which made **P59** a hybrid polymer of poly(*p*-phenylene vinylene) and poly(*p*-phenylene ethynylene). The alkoxy groups on the backbone endowed the functional copolymer highly solubility which was benefit for device fabrications. From size-exclusion chromatography characterization, **P59** showed high M_w of 16.2 kg/mol with polydispersity index (PDI) of 2.82. Compared to copolymers without pendant fullerenes, the excitation of **P59** in dilute toluene solution at 486 nm revealed that the photoluminescence was greatly quenched by 2 orders of magnitude, and which was caused by energy transfer from the photoexcited conjugated backbone to the fullerenes. Photoinduced absorption spectra of thin films indicated that a photoinduced electron-transfer reaction took place in the films, and the result indicated the migration of opposite charges to different sites in the films, which was similar to that observed in the polymer–fullerene blends system. Photovoltaic cells were prepared by spin coating **P59** from chloroform, and the device revealed promising characteristics with $J_{sc} = 0.42$ mA/cm^2, $V_{oc} = 0.83$ V, and a fill factor of 0.29 under white-light illumination (100 mW/cm^2, AM1.5).

Meanwhile, Janssen and co-workers [109] synthesized the poly(fluorene-alt-phenylene) bearing n-type perylenediimides (PDI) as pendant electron acceptor groups. Cyclic voltammetry experiments revealed the bipolar behavior of the copolymer, which combined both the good electron donor ability of the polymeric chain and the acceptor properties of the pendant PDI moieties. Solvent and temperature-dependent studies, together with the analysis of photoluminescence lifetimes, discovered photoinduced electron transfer from the electron-donating poly(fluorene-alt-phenylene) chain to the electron-accepting PDI pendant units and PDI aggregates. The property of photovoltaic devices based on this copolymer was not investigated.

Porphyrins have been recognized as the frequently employed building blocks of electron donors and sensitizers in artificial photosynthetic models for solar energy conversion [110]. The photoinduced electron-transfer processes between fullerenes and porphyrins have been intensively studied during past years [111, 112]. At the meantime, the phorphyrin derivatives showed well self-assembly properties and could controllably aggregated into well-defined nanostructures [113–117]. Due to these excellent properties, Li and co-workers [118–120] had designed and synthesized a series of double-cable copolymers based on fullerenes and porphyrins. In the polymerization processes, the monosubstituted acetylene with fullerene and porphyrin copolymerized under a very mild condition in the presence of transition metal catalyst $[Rh(nbd)Cl]_2$ in $CHCl_3$. Copolymer **P61** ($m1/m2 = 2/8$) were prepared with PDI of 1.3 and $M_n = 40{,}200$. Cyclic voltammetry were used to study the redox property of this copolymer, and it revealed four one-electron processes at -0.89, -1.40, -1.81, and -1.20 V, corresponding to the formation of monoanion, dianion, and trianion of fullerene moiety and the formation of porphyrin anion, respectively. Oxidation of the polymer took place in the potential range between 0.78 and 1.68 V, corresponding to the porphyrin cation. The photocurrent of **P61** film deposited on ITO electrode was measured under 21.2 mW cm^{-2} white-light irradiation. A steady and rapid cathodic 2.5 μA cm^{-2} photocurrent response was produced with prompt and reproducible response to on/off cycling. The aerobic incident-photon-to-photocurrent efficiency value was of 0.15% for true monolayer

coverage of **P61** at its peak absorption around 440 nm. These characters indicated the copolymers could be used in fabricating optoelectronic devices. Modified copolymer **P62** was also synthesized using same polymerization methods and the properties were investigated [119].

Copolymers containing phorphrins and fullerenes were further investigated in Li's group. The phorphrin moiety had been introduced into the backbone of copolymers containing poly(*p*-phenylenevinylene), and fullerenes were served as pendant groups [121]. Due to the strong π-conjugated system and steric hindrance, the series copolymers showed relatively low molecular weight. The cyclic voltammetry showed that **P63** and **P64** exhibited similar redox properties, and by the addition of metal, the redox properties of copolymers had been remarkably tuned. The photocurrent of the copolymers films deposited on ITO was measured separately under white-light irradiation of 20.7 mW/cm^2. The **P63** and **P64** films produced cathodic photocurrents of 0.149 and 0.152 μA/cm^2, respectively, which were greatly improved compared to **P65** (0.086 μA/cm^2). Moreover, films of **P66** and **P67** also showed enhanced photocurrent of 0.196 and 0.095 μA/cm^2, respectively. The results also indicated that this series of copolymers with pendent fullerene, porphyrin and PPV units were a good candidate for optoelectronic devices.

Li and co-workers [122] designed and prepared a soluble double-cable polythiophene with high content of C_{60} pendant. Prepared from precursor **P68**, the copolymer **P69** showed relatively high molecular weight in the range of 20–40 K, and bad solubility in THF due to the high content of C_{60}. The photophysical, electrochemical, and photovoltaic properties of **P69** were investigated and compared with its control polymer **P68**. **P69** exhibited the characteristic reduction peaks at -0.783, -1.187, and -1.651 V versus Ag/Ag$^+$, which indicated that the electronic properties of C_{60} was remained in the double-cable polymer. On the other hand, compared with that of **P68**, the increased onset oxidation potential of **P69** from 0.2 to 0.3 V could be ascribed to the steric hindrance of the big fullerene side chain. The absorption spectra indicated that there was no interaction between polythiophene backbone and C_{60} pendants at ground state, but photoluminescent spectra revealed the strong interaction at excited state. The AFM characterization indicated that films of **P69** were very smooth and uniform compared to that of **P68**/PCBM blends. The maximum PCE of the polymer solar cell based on **P69** was about 0.52% under AM 1.5, 100 mW/cm^2, which was five times higher than that of the device based on **P68** blended with $PC_{61}BM$ (0.10%) in same condition. The efficiency of 0.52% was high value for the PSCs based on the double-cable polymers.

Although, double-cable copolymers can insure the intimate contact between acceptor and donor segments in molecular heterojunction and the maximum interfacial area will be produced, the maximum PCE of the PSC based on this kind of copolymers is comparable lower than traditional blended BHJ solar cells. The best value for a double-cable polymer ever reported is no more than 1%. It can be easily understood that it may be the uniform molecular heterojunction that results in the increased charge recombination and inefficient charge transportation in the active layer, and that accounts for the poorer PCE of double-cable copolymers compared with the blended BHJ solar cells.

Metal atom containing copolymers

Except for the introduction of donor and acceptor moieties to straightly tune the absorption property in solar irradiance, the lifetime of excited state also can be designable by introducing heavy metal atoms in the conjugated copolymers. It is well-known that the lifetime of triplet excited states is normally 3 orders of magnitude longer than the nanosecond decay of singlet excited states in conjugated copolymers. The prolonged lifetime of excited state is benefit for charge separation and charge transfer in the solid film in a long distance. Compared with normal polymers, the triplet-forming polymers showed increased exciton diffusion length in the photovoltaic devices due to the forbidden nature of recombination from the triplet states [123]. This means that the design of materials with high triplet yields may offer an efficient access to benefit the charge transportation and collection and increase the I_{oc} for solar cells [124].

The extensively conjugated two-dimensional π-system endows porphyrins suitable properties in light-harvesting and efficient electron transfer because the uptake or release of electrons results in minimal structural change [125]. Moreover, porphyrins have extensive absorption over the wavelengths of the solar spectrum [126]. Wong and co-workers [127] introduced metalloporphyrins block into polyplatinynes linear-conjugated systems for the construction of new p-type photovoltaic active materials. In these systems, the thiophene and phenyl groups were adopted to extend the π-conjugation and cover the missing absorption region (430–530 nm) or enhance the absorption of the weaker Q-bands. The experiment and computation methods were combined to investigate the molecular structure and HOMO and LUMO energy levels for **P70**–**P72**. Cyclic voltammetry indicated that the Pt/Zn mixed metal polymers had HOMO energy level at −5.53 to −5.62 eV and LUMO energy level at −3.64 to −3.73 eV. From absorption spectra, it was calculated that the optical band gaps ranged from 1.93 to 2.02 eV for **P70**–**P72**. BHJ solar cells with metallopolymers/PCBM (1:4) as active layer were studied under illumination of an AM 1.5 solar cell simulator, and PCE of 0.68, 0.71, and 1.04%, respectively, were obtained from **P70** to **P72**. The metallopolymer **P72** showed the highest PCE, V_{oc} of 0.77 V, J_{sc} of 3.42 mA cm^{-2}, and fill factor of 0.39. This study represents the first example of porphyrin-containing polymetallaynes used for harvesting solar energy in solution-processed photovoltaic devices.

Jenekhe and co-workers [128] synthesized and investigated a series of organometallic D–A-conjugated polymer semiconductors. The polyplatinynes copolymers showed reversible electrochemical reduction waves from which electron affinities were found to be 2.95–3.28 eV. From the onset oxidation potentials of the polymers, ionization potentials were determined to be 4.82–5.23 eV. The absorption spectra of solid films were finely tuned in the visible and near-infrared regions by changing the composition. Moreover, the optical band gaps of the D–A polymers were modified from 1.49 to 1.97 eV. From the FET characterization, the polymer thin films showed p-channel field-effect charge transport with hole mobilities of 3.87×10^{-7}–3.32×10^{-5} cm^2/(V s). BHJ solar cells based on blends of the copolymers/$PC_{71}BM$ with film thickness in range of 60–80 nm obtained PCE of 2.41% for **P73**, 0.68% for **P74**, 0.36% for **P75**, 0.016%

for **P76**, and 0.32% for **P77**. The poor PCE of **P76** was due to the low V_{oc} (0.39 V), J_{sc} (0.25 mA/cm^2), and fill factor (0.17). However, the investigations provide us an efficient method for designing optical band gap and photovoltaic properties of organometallic-conjugated polymer semiconductors.

The effective conjugation length plays an intensive role in controlling the solar cell efficiency. In polyplatinynes, the poor energetic overlap between the 5*d* Pt and 2*p* C orbitals limited the effective conjugation length compared to structurally analogous poly(phenylene ethynylenes) [129]. Moreover, the decreased effective conjugation length not only influence the absorption spectra but also prohibit the exciton localization and exciton diffusivity, and ultimately limited the photovoltaic performance even if long-lived triplets are realized [130].

Different from polyplatinynes, Fréchet and co-workers [130] built a novel kind of platinum-containing conjugated copolymer, in which the platinum atom was attached to the conjugated backbone via a C^N ligand. The C^N ligand can produce the coplanar conformation of the monomer and the O^O diketonate ligand also can improve the solubility of the copolymers. **P78** and **P79** were prepared using Stille and Suzuki, respectively, and by copolymerizing with different monomers, the optical band gaps were tuned between 2.1 and 1.65 eV. Both in solution and in solid films, the absorption spectra of the copolymers showed one strong transition at approximately 350 nm which was attributed to the direct excitation of the metal complex, and one strong transition at longer wavelength derived from excitations delocalized along the conjugated polymer chain. Triplet exciton formation was studied indirectly by measuring photosensitized emission of singlet oxygen in both solution and in film. The ability of the materials to sensitize formation of singlet oxygen varies both with excitation wavelength and with the change from solution to solid state. The photovoltaic performances of **P78** and **P79** were also detected in preliminary experiments with PCE of 1.3 and 0.40%, respectively, obtained from a BHJ cell based on polymer/PCBM blends under AM 1.5 illumination at 100 mW/cm. The **P78** solar cells showed better performance than that of **P79**, which was partly due to its superior overlap with the solar spectrum and the possibly localized holes in **P79** which limited charge transport in a device.

Schulz and Holdcroft [123] synthesized copolymer **P80** and **P81** using Suzuki polycondensation, and investigated the effect of incorporating an iridium complex into a π-conjugated polymer backbone on photovoltaic properties such as charge generation, PCE and EQE. The characterization was performed using NMR, UV–Vis, photoluminescence, and time-resolved luminescence spectroscopy gel permeation chromatography; elemental analysis; and photovoltaic devices. The EQE of **P81** showed an absolutely increase from 1.1 to 10.3 over **P80**, and this was attributed to the formation of triplet state in **P81**, and longer diffusion lengths of the triplet exciton in **P81** compared with singlet exciton in **P80**. Photovoltaic devices were fabricated by blending **P80** and **P81** with PCBM. Although, the solar PCE based on **P80** and **P81** were both much lower than normal solar cells, devices based on **P81** exhibited an obviously improved device performance. The J_{sc} were 0.01 and 0.44 mA/cm^2 for devices based on **P80** and **P81**, respectively, and the PCE was greatly improved from 0.002 for **P80** to 0.07% for **P81**.

Block copolymers used for photovoltaic devices

For the BHJ solar cells, the microphase structures between donor and acceptor play intensive influence in controlling the device efficiency. Optimization of the nanoscale morphologies can maximize the charge separation, transfer and collection [4, 131]. After the photoexcitation of electron-donating component, the charge separation takes place and the electrons and holes are transferred to the electrodes through the donor and acceptor domains. Moreover, the lifetime of photogenerated excitons are just on the order of ps–ns, and the maximum diffusion distance is about 10 nm [132]. This indicates that abundant of D–A interfaces must be needed for charge separation. It is found that the patterned structures with continuous and straight pathway are propitious to charge transfer [133–135]. Therefore, during the processes of the charge separation and charge transfer, the microphase structures of the active layer play great important role in tuning these processes. During past decade, the nano-fabrication technologies such as organic vapor–solid phase reaction [136, 137], template methods [138–141], self-assembly, and self-polymerization [142], have been well developed, and also many appropriate efforts have been applied in optimizing the microphase structures between donor and acceptor blends, such as annealing [9, 10], spin-coating speed [11, 12], solvent treatment [13–16], and so on. For example, a CdS-PPY single axial organic/inorganic p–n junction nanowire was used to construct the organic/inorganic hybrid solar cells on the nanoscale for understanding the effect of interface structure on the photovoltaic performance. [143] As shown in Fig. 29a, excitons generated by the light reach the hybrid interface from the CdS side and effectively dissociate at the interface of CdS-PPY. The electrons and holes generated in this process could also transport through CdS and PPY, respectively, which generates the photocurrent efficiently in the CdS-PPY p–n junction nanowire. Most of the CdS-PPY axial p–n nanowire solar cell devices have efficiency around 0.016% under an illumination intensity of 6.05 mW/cm^2, and the maximum efficiency is up to 0.018% under the same illumination intensity (6.05 mW/cm^2). Neither the CdS nanowire nor the PPY nanowire shows power generation under the same condition (Fig. 29d, e), indicating that the photovoltaic properties were characteristic of a CdS-PPY nanowire. This is the first example for generating photovoltaic response on a single heterojuction wire that is not observed from the independent components. However, to obtain the 10 nm length scale patterned films is very difficult for these traditional techniques, including the lithographic methods. Moreover, the reproducibility and stability of the solar cell devices is poor because of the microphase separation of the polymer/PCBM blends active layer [144–146].

During the past decades, the self-assembly properties of block copolymers had been well studied, and block copolymers offered great superiorities in controlling the self-assembly nanostructures, especially for patterned nanostructures in 10 nm length scale. Moreover, the size and morphologies of the patterned nanostructures can be controlled by tuning the molecular weight and the structures of the block copolymers [147, 148]. Block copolymers self-assembly may be used to create patterned active layer for optimized charge separation, charge mobility, and

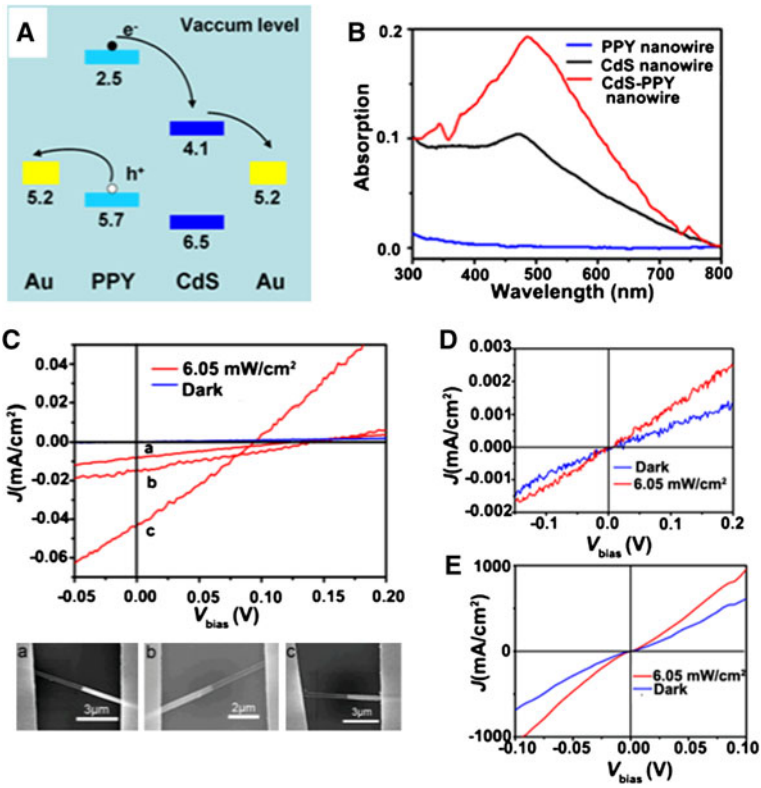

Fig. 29 **a** Energy level diagram of a CdS-PPY nanowire. **b** UV–Vis absorption spectra of CdS-PPY p–n junction nanowires, CdS nanowire, and PPY nanowire. **c** Dark/light current density versus applied voltage bias (*J*–*V*) data of typical single CdS-PPY nanowire solar cells with device lengths of 7.428 (*a*), 6.922 (*b*), and 6.597 μm (*c*). Dark/light *J*–*V* data of CdS nanowire device (**d**), PPY nanowire device (**e**). Reproduced with permission from Ref. [143]. Copyright 2010 American Physical Society

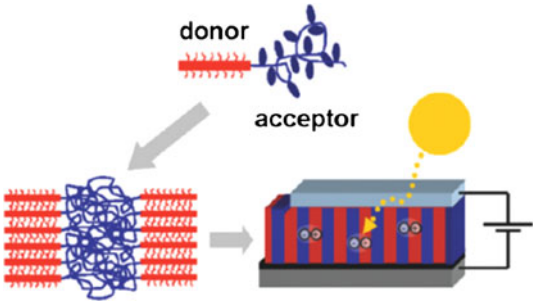

Fig. 30 The feature of solar cell based on block copolymers. Reproduced with permission from Ref. [146]. Copyright 2009 American Physical Society

collection on the characteristic 10 nm length scale of exciton diffusion [149] (Fig. 30).

In order to develop high-performance polymer-based solar cell devices, it is necessary to construct the active layer with highly ordered nanoscale morphologies.

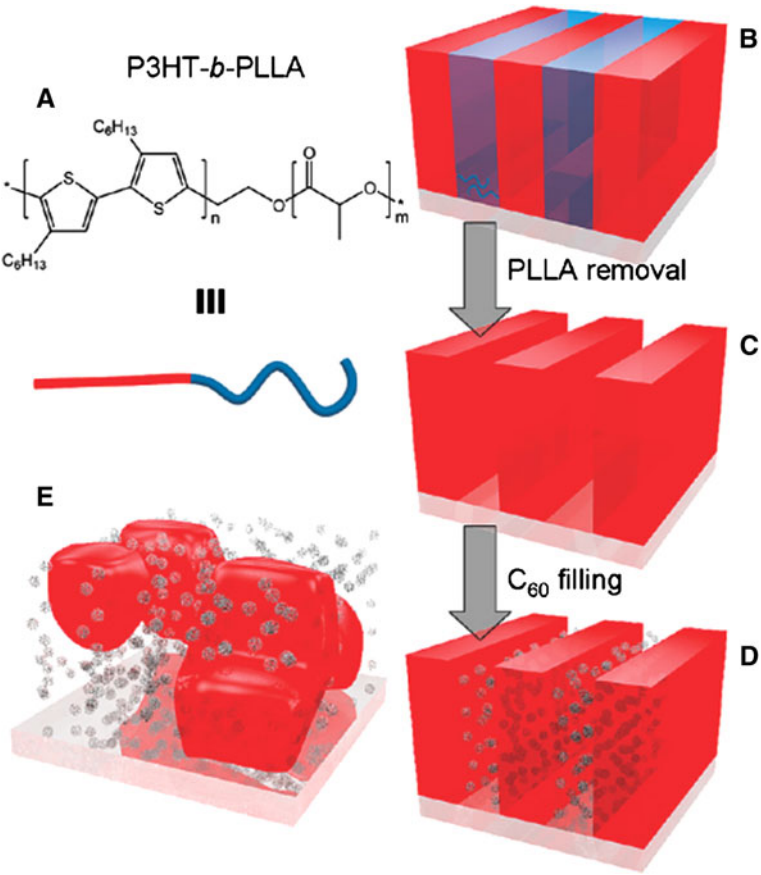

Fig. 31 The assembly structure of P3HT-*b*-PLLA and possible application in solar cell. Reproduced with permission from Ref. [150]. Copyright 2009 American Physical Society

Botiz and Darling [150] designed and developed an ordered nanoscale morphology from poly(3-hexylthiophene)-*block*-poly(L-lactide) (P3HT-*b*-PLLA), which was used both as an active materials and as a structure-directing agent to pattern C_{60} derivative (Fig. 31). The P3HT block is selected because of the outstanding charge carrier mobility and suitable band gap in the visible region [151, 152]. The microphase separation process produces the patterned films and the biodegradable PLLA block can be readily removed under basic condition [153]. The AFM and TEM characterizations indicate that the well-patterned films can be easily prepared by self-assembly. Moreover, the patterned films removed away from PLLA were served as the vessels for acceptor materials (C_{60}) and the new alternating D–A nanostructures domains were produced. Using this morphological control method, the structure–property relationships with unprecedented detail with the ultimate goal of maximizing the performance of future organic/hybrid PV devices can be probed.

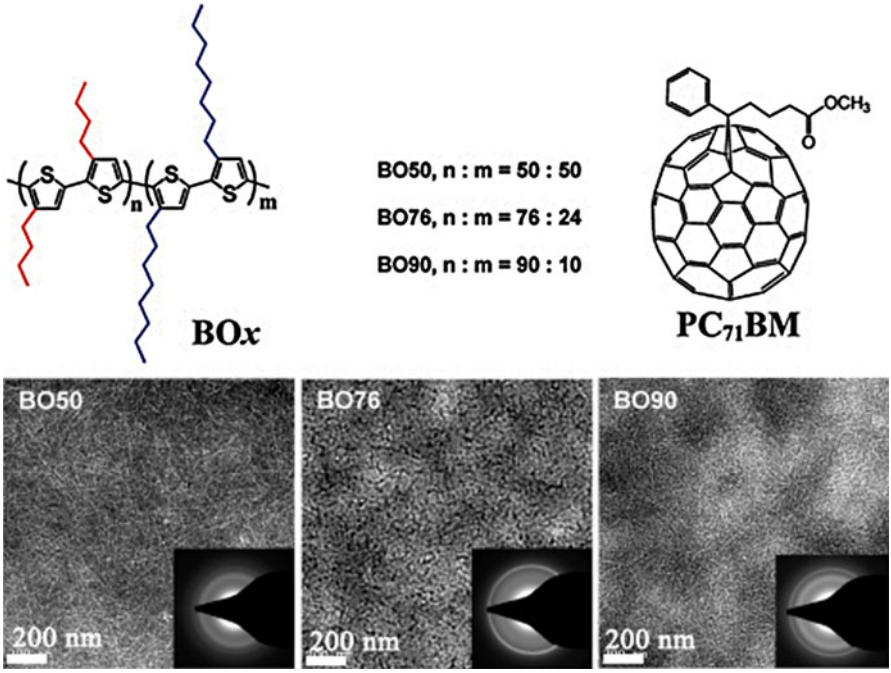

Fig. 32 Structures of the diblock copoly(3-alkylthiophene)s, BO*x*, and $PC_{71}BM$; TEM images of BO*x* NWs:PC_{71} BM thin films peeled from solar cells and their SAED patterns (*inset*). Reproduced with permission from Ref. [154]. Copyright 2011 American Physical Society

Block copolymers show great advantages in controlling the nanostructures compared to homopolymers, and the size of domains can be tuned by changing the molecular structures. Jenekhe and co-workers [154] investigated the self-assembly properties of diblock copolymer semiconductor poly(3-butylthiophene)-*block*-poly(3-octylthiophene) (BO*x*) and their application in solar cell. By tuning the block copolymer compositions, BO*x* can aggregate into crystalline nanowires with similar width (13–16 nm) and a tunable aspect ratio (length/width) of 50–260 by solution-phase self-assembly in *o*-dichlorobenzene. Moreover, the nanowires morphologies in polymer/PCBM active layer were illustrated in Fig. 32. The width of block copolymers nanowires was comparable to the exciton diffusion length in polymer-based photovoltaic devices. Tunable aspect ratio of nanowires indicated that the diblock copolymer composition provides a facile and powerful means for tuning the aspect ratio of polymer semiconductor nanowires. The photovoltaic properties of BO*x* NWs in BHJ solar cells were studied by blending the NWs with the electron acceptor, $PC_{71}BM$, using the device structure: ITO/PEDOT:PSS/active layer/LiF/Al. The solar cells were characterized under AM1.5 solar illumination at 1 sun (100 mW/cm^2) in laboratory air, and it was indicated that the photovoltaic efficiency increased with increasing aspect ratio, reaching 3.4% at the highest average aspect ratio of 260. The enhancement of photovoltaic efficiency with

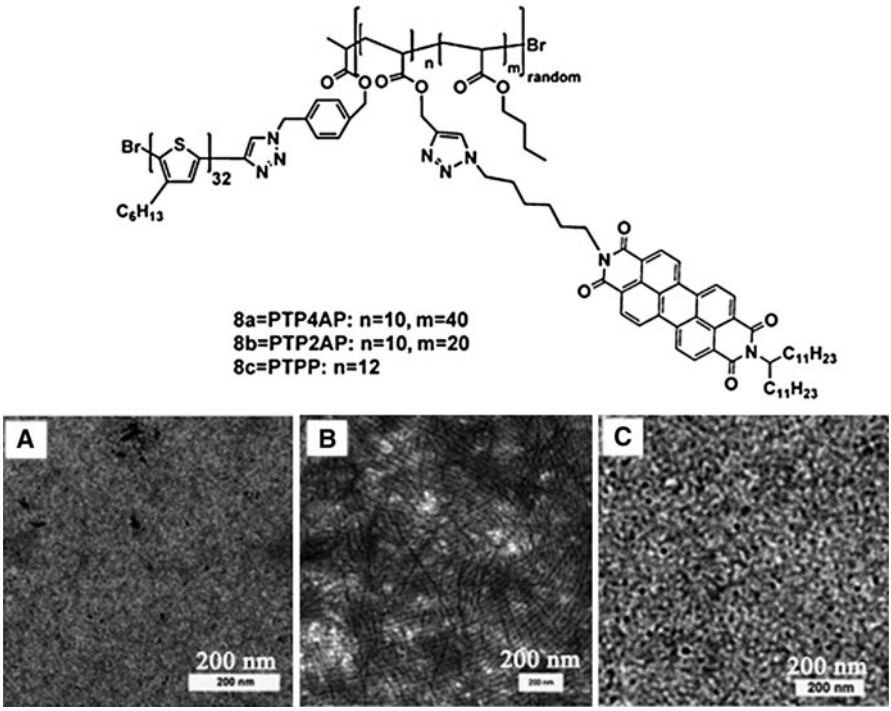

Fig. 33 The molecular structure of block copolymers and TEM plane view images of P3HT–PTP4AP with **a** disordered structures, **b** long range order, and **c** poorly organized nanostructures. Reproduced with permission from Ref. [155]. Copyright 2009 Royal Society of Chemistry

increasing aspect ratio of NWs was explained in terms of increased exciton and charge photogeneration and collection in the BHJ solar cells.

Self-assembly of copolymers with donor block shows a promising pathway to control the morphologies of donor domains and fabricate the solar cells. Meanwhile, more and more groups pay attention to synthesize the block copolymers with both donor and acceptor blocks, and the self-assembly of this kind of block copolymer provides an effective method to fabricate solar cell with D–A alternating domain structures, which may show optimized device performance. Segalman and co-workers [155] combined the atom transfer radical polymerization and "click chemistry" methods to synthesize a series of rod-coil diblock copolymers, in which the rod poly(3-hexylthiophene) (P3HT) served as the donor block and the coil segment contained the electron-deficient perylenediimides (Fig. 33). Block copolymer films with disordered structure, long range order and poorly organized nanostructures, respectively, were obtained by controlling the casting speeds. Devices with active layers which were completely disordered (molecularly mixed), contain short range order in which the nanodomains were molecularly pure, but were poorly organized, or consisted of cylindrical fibrils with their long axes running parallel to the electrodes were compared. Active layers with well formed but poorly organized nanodomains had the highest photovoltaic efficiencies

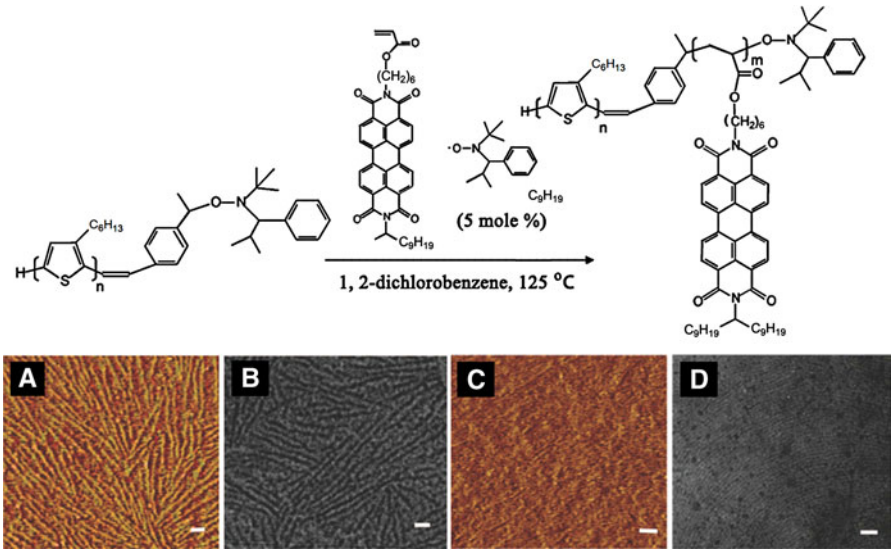

Fig. 34 Chemical structure of diblock copolymers and assembly structure. **a** SFM phase image and **b** TEM image of block copolymer thin film (from a 1 wt% toluene solution at 2,500 rpm) after annealing. **c** SFM phase image and **d** TEM image of drop-cast block copolymer film from 0.1 wt% toluene solution on Si substrate. *Scale bar* 100 nm. Reproduced with permission from Ref. [156]. Copyright 2009 American Physical Society

indicating that molecular scale segregation has a significant effect on device performance. The poor performance of the well-defined cylindrical nanostructures is probably a reflection of the poor charge-transport properties associated with the misorientation of the long axes parallel to the electrodes.

Combining Grignard metathesis polymerization and nitroxide-mediated polymerization methods, Emrick and co-workers [156] synthesized the similar D–A diblock copolymers, composed of regioregular poly(3-hexylthiophene) (rrP3HT) as the electron donor block and poly(perylene diimide acrylate) as the electron acceptor block. The diblock copolymers were prepared with low-to-moderate polydispersity indices (1.2–1.4) and sufficiently high molecular weights for spin-coating. The efficient photoluminescence quenching in solid films indicated the efficient charge separation. The solar cells containing the as-spun films showed PCE about 0.11%. After thermal annealing, devices exhibited fibrillar morphology with long range order (Fig. 34), and obtained significantly higher PCE about 0.49%. This post-annealing increase PCE due to the increased short-circuit current and only slight decrease in the open-circuit voltage. SFM, TEM, and X-ray diffraction characterization all indicated that the increased short-circuit current would arise from a reorientation and enhanced ordering of the copolymer during annealing, which would facilitate charge transport [156]. From Fig. 33b–d, it is clearly enounced that the assembly phase structures of active layers are efficiently controlled by tuning the diblock copolymer composition.

Fullerene derivatives are considered as the most promising electron acceptors in polymer-based photovoltaic devices. D–A diblock copolymers containing the

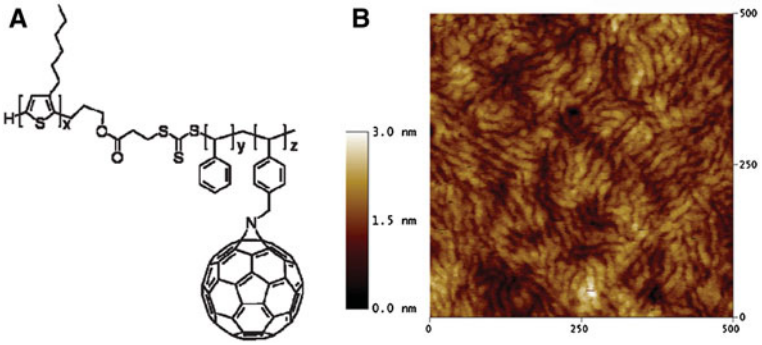

Fig. 35 **a** Chemical structure of the P3HT-*b*-P($S_{89}BAz_{11}$)-C_{60} rod–coil copolymer where $x = 1$, $y = 7.6$, and $z = 1.4$; **b** surface-topographic image of the triblock-copolymer film spin-coated from chlorobenzene solution onto an ITO-coated glass substrate. Reproduced with permission from Ref. [157]. Copyright 2010 Wiley-VCH Verlag GmbH & Co. KGaA

fullerene pendant groups greatly expand the block copolymer application in solar cells. Nguyen and co-workers [157] have synthesized and characterized the morphological and charge-transport properties of P3HT-*b*-P($S_{89}BAz_{11}$)-C_{60} (Fig. 35). UV–Visible (UV–Vis) measurements of films show characteristic absorptions from both P3HT and C_{60}. Quenching of photoluminescence indicated that the P3HT and fullerene blocks are in intimate contact to facilitate charge separation. Morphology, phase, and photo- and dark-current images from scanning probe studies confirmed the presence of nanoscale phase segregation. The fibers appear to consist of the conjugated-rod block surrounded by the fullerene- and styrene coil blocks. *I–V* characteristics measured by conducting AFM indicate that the film is fairly electrically homogenous and that the hole and electron mobilities are comparable to those of P3HT: PCBM BHJ films. The results support that P3HT-*b*-P($S_{89}BAz_{11}$)-C_{60} may provide the optimal morphology for BHJ solar cells without the need for thermal or solvent annealing or adding additives. Space–charge limited current behavior, where $J \propto V^2$and $J \propto L^{-3}$ is observed in both diodes, allows the determination of carrier mobilities. The hole and electron mobilities calculated from this data are 2.7×10^{-5} and 1.7×10^{-6} $cm^2/(V\ s)$, respectively. These values are slightly lower than mobility values reported for P3HT:PCBM BHJ measured using the same technique.

With the objective of enhancing photovoltaic performance, a D–A, rod-coil diblock copolymer based on poly(*p*-phenylenevinylene) (PPV) and fullerene was prepared in Hadziioannou and co-workers [158], and the microphase separation property was investigated. Diblock copolymers were obtained by using an end-functionalized PPV as a macroinitiator for the nitroxide-mediated controlled radical polymerization of a roil block. The latter block was subsequently functionalized with C_{60} through atom transfer radical addition. The molecular structure was shown in Fig. 36. Upon casting from CS_2 solution, films exhibited micrometer-scale, honeycomb-like patterns in Fig. 36a, b. From the luminescence image (Fig. 36b), it was concluded that the luminescence intensity was very low in PPV-*b*-PSFu compared with that of PPV-*b*-PS film, and it was indicated that the luminescence of

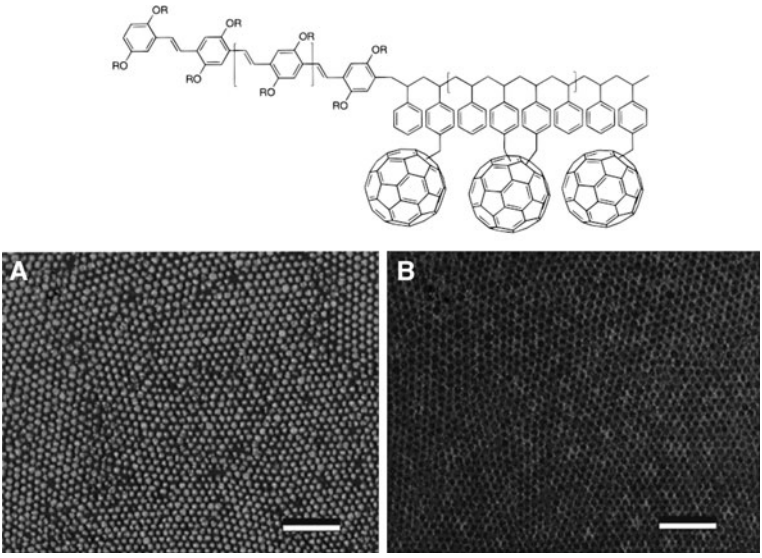

Fig. 36 Molecular structure of copolymer PPV-*b*-PSFu and optical transmission (**a**) and luminescence (**b**) micrographs of honeycomb structures in solution-cast films of PPV-b-PSFu. *Scale bars* 20 μm. Reproduced with permission from Ref. [158]. Copyright 2000 American Physical Society

PPV was efficiently quenched and efficient electron transfer to pendant C_{60} side groups occurred.

With small adjustment, Heiser and co-workers [159] synthesized similar copolymers with PPV-*b*-PSFu (Fig. 37). Material properties were explored by X-ray diffraction, AFM, UV–Vis absorption, and photoluminescence spectroscopy. The AFM phase images of Fig. 37a, b exhibited that uniform lamella structures were prepared from fullerene-free copolymer **1a** and **1b**, and by the addition of fullerene the uniform lamella structures were remarkably interrupted through the growth of fullerene micro domains. Moreover, the AFM phase images also indicated that the consecutive D–A nanodomains were obtained in the fullerene-containing block copolymer **2** thin films and the D–A interface were greatly increased. Similar with the results obtained from AFM, the strong photoluminescence quenching further suggested the presence of a large D–A interface and the efficient exciton dissociation took place at the D–A interface. Although, increased D–A interface were prepared, the resulting active layers based on fullerene-containing block copolymer **2** were not used to build efficient BHJ photovoltaic device.

Although, many photovoltaic devices based on block copolymers just obtained lower efficiency than traditional BHJ solar cells, block copolymer design strategies still may be a very promising pathway to optimize photovoltaic device performance by controlling the phase structure of the active layer on the exciton diffusion length scale (10 nm) while also providing suitable morphologies for charge transport. More studies on block copolymer synthesis and device formation are still necessary to prove the utility of block copolymers in photovoltaic devices, to understand the

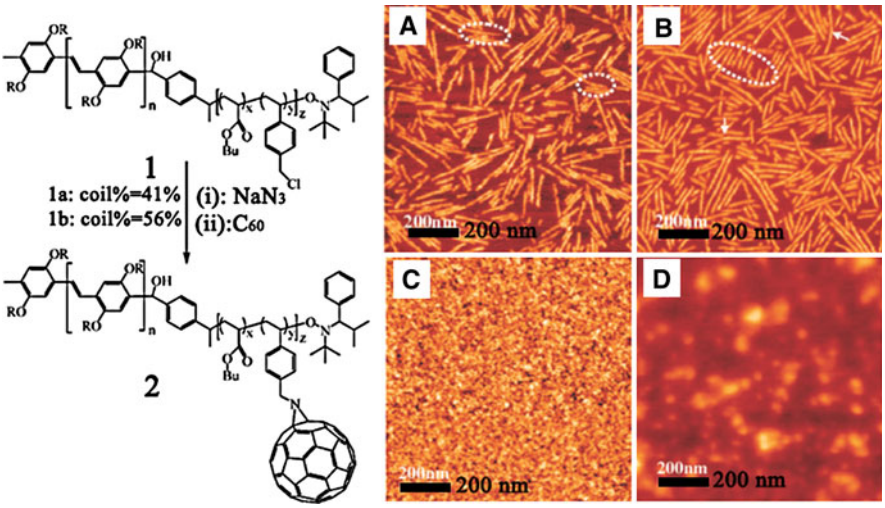

Fig. 37 The molecular structure and AFM phase images of **a** as-deposited fullerene-free copolymer **1a**, **b** as-deposited copolymer **1b**, **c** as-deposited fullerene-containing copolymer **2**, **d** copolymer **2** after 1 h at 90 °C. Reproduced with permission from Ref. [159]. Copyright 2008 American Physical Society

role of patterned morphology on device performance and to provide the efficient guideline to design novel functional copolymers.

Conclusion

By the intensive studies and development of process technology, the PCE of polymeric photovoltaic devices will be greatly improved and the devices will show promising applications in solving energy crisis. In this view, it is concluded that molecular design strategies provide us efficient pathways to achieve functional polymers with many optimized properties, such as suitable band gap energy, the optimized self-assembly morphologies, good solution-processability as well as the hole mobility of the solid films. By combination of electron-rich and electron-deficiency moieties, the copolymers consisting of D–A alternating structures can obtain appropriate band gap energy, which increases the absorption efficiency with large V_{oc}. By introduction of metal atoms in functional copolymers, the lifetime of excited state can be elongated about 3 orders of magnitude longer than normal π-conjugated copolymers, and the prolonged lifetime is benefit for charge separation and charge transfer in the solid film with increased exciton diffusion length. The double-cable copolymers and block copolymers provide us another efficiency method to increase the D–A interface and obtain controllable microphase morphologies which also can benefit for the charge dissociation and transport.

Although, there are too many factors of device fabrication that can influence the solar cells performance, it is possible to prepare BHJ photovoltaic device with broad

absorption in the visible range, well-patterned microphase morphologies in the exciton diffusion length scale (10 nm) adopting these molecular design strategies. The low-cost polymer photovoltaic devices with exciting efficiencies may be produced when these molecular design strategies are efficiently combined together, and this makes the possibility of commercially available PSCs come true.

Acknowledgments We appreciate Prof. Yuliang Li and Dr. Huibiao Liu for their helpful discussion. This study was supported by the National Nature Science Foundation of China (21031006, 20831160507, 20721061, 20971127) and the National Basic Research 973 Program of China.

References

1. Halls JJM, Pichler K, Friend RH, Moratti SC, Holmes AB (1996) Exciton diffusion and dissociation in a poly(*p*-phenylenevinylene)/C[sub 60] heterojunction photovoltaic cell. Appl Phys Lett 68: 3120–3122
2. Haugeneder A, Neges M, Kallinger C, Spirkl W, Lemmer U, Feldmann J, Scherf U, Harth E, uuml, gel A, llen K (1999) Exciton diffusion and dissociation in conjugated polymer/fullerene blends and heterostructures. Phys Rev B 59:15346
3. Wöhrle D, Meissner D (1991) Organic solar cells. Adv Mater 3:129–138. doi:10.1002/adma.19910030303
4. Yu G, Gao J, Hummelen JC, Wudl F, Heeger AJ (1995) Polymer photovoltaic cells: enhanced efficiencies via a network of internal donor–acceptor heterojunctions. Science 270:1789–1791. doi:10.1126/science.270.5243.1789
5. Günes S, Neugebauer H, Sariciftci NS (2007) Conjugated polymer-based organic solar cells. Chem Rev 107:1324–1338. doi:10.1021/cr050149z
6. Heremans P, Cheyns D, Rand BP (2009) Strategies for increasing the efficiency of heterojunction organic solar cells: material selection and device architecture. Acc Chem Res 42:1740–1747. doi:10.1021/ar9000923
7. Scherf U, Gutacker A, Koenen N (2008) All-conjugated block copolymers. Acc Chem Res 41:1086–1097. doi:10.1021/ar7002539
8. Westenhoff S, Howard IA, Hodgkiss JM, Kirov KR, Bronstein HA, Williams CK, Greenham NC, Friend RH (2008) Charge recombination in organic photovoltaic devices with high open-circuit voltages. J Am Chem Soc 130:13653–13658. doi:10.1021/ja803054g
9. Gu ZJ, Kanto T, Tsuchiya K, Shimomura T, Ogino K (2011) Annealing effect on performance and morphology of photovoltaic devices based on poly(3-hexylthiophene)-*b*-poly(ethylene oxide). J Polym Sci A 49:2645–2652. doi:10.1002/pola.24696
10. Yin W, Dadmun M (2011) A new model for the morphology of P3HT/PCBM organic photovoltaics from small-angle neutron scattering: rivers and streams. ACS Nano 5:4756–4768. doi:10.1021/nn200744q
11. Tsai YS, Chu WP, Juang FS, Tang RM, Chang MH, Hsieh TE, Liu MO (2011) Efficiency improvement of organic solar cells by slow growth and changing spin-coating parameters for active layers. Jpn J Appl Phys 50:022301–022304. doi:10.1143/jjap.50.022301
12. Ebbens S, Hodgkinson R, Parnell AJ, Dunbar A, Martin SJ, Topham PD, Clarke N, Howse JR (2011) In situ imaging and height reconstruction of phase separation processes in polymer blends during spin coating. ACS Nano 5:5124–5131. doi:10.1021/nn201210e
13. Bo P, Xia G, Chaohua C, Yingping Z, Chunyue P, Yongfang L (2011) Performance improvement of polymer solar cells by using a solvent-treated poly(3,4-ethylenedioxythiophene):poly(styrenesulfonate) buffer layer. Appl Phys Lett 98:243308. doi:10.1063/1.3600665
14. Salim T, Wong LH, Brauer B, Kukreja R, Foo YL, Bao ZN, Lam YM (2011) Solvent additives and their effects on blend morphologies of bulk heterojunctions. J Mater Chem 21:242–250. doi:10.1039/c0jm01976c
15. Xia YJ, Ouyang JY (2011) PEDOT:PSS films with significantly enhanced conductivities induced by preferential solvation with cosolvents and their application in polymer photovoltaic cells. J Mater Chem 21:4927–4936. doi:10.1039/c0jm04177g

16. Kim JS, Lee JH, Park JH, Shim C, Sim M, Cho K (2011) High-efficiency organic solar cells based on preformed poly(3-hexylthiophene) nanowires. Adv Funct Mater 21:480–486. doi:409335753,12,1
17. Coakley KM, McGehee MD (2004) Conjugated polymer photovoltaic cells. Chem Mater 16:4533–4542. doi:10.1021/cm049654n
18. Fan Z, Razavi H, Do J-W, Moriwaki A, Ergen O, Chueh Y-L, Leu PW, Ho JC, Takahashi T, Reichertz LA, Neale S, Yu K, Wu M, Ager JW, Javey A (2009) Three-dimensional nanopillar-array photovoltaics on low-cost and flexible substrates. Nat Mater 8:648–653
19. Coakley KM, McGehee MD (2003) Photovoltaic cells made from conjugated polymers infiltrated into mesoporous titania. Appl Phys Lett 83:3380–3382
20. Gao H, Chen YX, Luo Y (2011) Three-dimensional nano-networked P3MT/PCBM solar cells. Nanotechnology 22:285203. doi:10.1088/0957-4484/22/28/285203
21. Zhu M, Zhou CJ, Zhao YJ, Li YJ, Liu HB, Li YL (2009) Synthesis of a fluorescent polymer bearing covalently linked thienylene moieties and rhodamine for efficient sensing. Macromol Rapid Commun 30:1339–1344. doi:10.1002/marc.200900210
22. Lv J, Ouyang CB, Yin XD, Zheng HY, Zuo ZC, Xu JL, Liu HB, Li YL (2008) Reversible and highly selective fluorescent sensor for mercury(II) based on a water-soluble poly(para-phenylene)s containing thymine and sulfonate moieties. Macromol Rapid Commun 29:1588–1592. doi:10.1002/marc.200800256
23. Li CH, Zhou CJ, Zheng HY, Yin XD, Zuo ZC, Liu HB, Li YL (2008) Synthesis of a novel poly (para-phenylene ethynylene) for highly selective and sensitive sensing mercury (II) ions. J Polym Sci A 46:1998–2007. doi:10.1002/pola.22534
24. Li CH, Guo YB, Lv J, Xu JL, Li YL, Wang S, Liu HB, Zhu DB (2007) Induced helix formation and stabilization of a meta-linked polymer containing pyridine units. J Polym Sci A 45:1403–1412. doi:10.1002/pola.21910
25. Liu Y, Deng CM, Tang L, Qin AJ, Hu RR, Sun JZ, Tang BZ (2011) Specific detection of D-glucose by a tetraphenylethene-based fluorescent sensor. J Am Chem Soc 133:660–663. doi:10.1021/ja107086y
26. Liu JZ, Zhong YC, Lam JWY, Lu P, Hong YN, Yu Y, Yue YN, Faisal M, Sung HHY, Williams ID, Wong KS, Tang BZ (2010) Hyperbranched conjugated polysiloles: synthesis, structure, aggregation-enhanced emission, multicolor fluorescent photopatterning, and superamplified detection of explosives. Macromolecules 43:4921–4936. doi:10.1021/ma902432m
27. Fang HJ, Xiao SX, Li YL, Xiao SQ, Li HM, Liu HB, Shi ZQ, Zhu DB (2003) Synthesis and characterization of a C-60 covalently linked poly(phenylenevinylene) derivative containing trimethylsilyl pendant. Synth Met 135:837–838. doi:10.1016/s0379-6779(02)00922-0
28. Wang S, Yang JL, Li YL, Lin HZ, Guo ZX, Xiao SX, Shi ZQ, Zhu DB, Woo HS, Carroll DL, Kee IS, Lee JH (2002) Composites of C-60 based poly(phenylene vinylene) dyad and conjugated polymer for polymer light-emitting devices. Appl Phys Lett 80:3847–3849. doi:10.1063/1.1480881
29. Wang S, Xiao SX, Li YL, Shi ZQ, Du CM, Fang HJ, Zhu DB (2002) Synthesis and characterization of new C-60-PPV dyads containing carbazole moiety. Polymer 43:2049–2054. doi:10.1016/s0032-3861(01)00795-9
30. Xiao SX, Wang S, Fang HJ, Li YL, Shi ZQ, Du CM, Zhu DB (2001) Synthesis and characterization of a novel class of PPV derivatives covalently linked to C-60. Macromol Rapid Commun 22:1313–1318. doi:10.1002/1521-3927(20011101)22:16<1313:aid-marc1313>3.0.co;2-y
31. Liu Y, Yang CH, Li YJ, Li YL, Wang S, Zhuang JP, Liu HB, Wang N, He XR, Li YF, Zhu DB (2005) Synthesis and photovoltaic characteristics of novel copolymers containing poly(phenylenevinylene) and triphenylamine moieties connected at 1,7 bay positions of perylene bisimide. Macromolecules 38:716–721. doi:10.1021/ma0484911
32. Jiu T, Li Y, Liu X, Liu H, Li C, Ye J, Zhu D (2007) Molecular modeling of poly(*p*-phenylenevinylene): Synthesis and photophysical properties of oligomers. J Polym Sci A 45:911–924. doi:10.1002/pola.21862
33. Cheng YJ, Yang SH, Hsu CS (2009) Synthesis of conjugated polymers for organic solar cell applications. Chem Rev 109:5868–5923. doi:10.1021/cr900182s
34. Wu J-S, Cheng Y-J, Dubosc M, Hsieh C-H, Chang C-Y, Hsu C-S (2010) Donor–acceptor polymers based on multi-fused heptacyclic structures: synthesis, characterization and photovoltaic applications. Chem Commun 46:3259–3261
35. Zhang F, Mammo W, Andersson LM, Admassie S, Andersson MR, Inganäs O (2006) Low-bandgap alternating fluorene copolymer/methanofullerene heterojunctions in efficient near-infrared polymer solar cells. Adv Mater 18:2169–2173. doi:10.1002/adma.200600124

36. Cho SY, Grimsdale AC, Jones DJ, Watkins SE, Holmes AB (2007) Polyfluorenes without monoalkylfluorene defects. J Am Chem Soc 129:11910–11911. doi:10.1021/ja074634i
37. Schulz GL, Chen XW, Holdcroft S (2009) High band gap poly(9,9-dihexylfluorene-alt-bithiophene) blended with 6,6-phenyl C-61 butyric acid methyl ester for use in efficient photovoltaic devices. Appl Phys Lett 94:023302. doi:02330210.1063/1.3070574
38. Tang W, Ke L, Tan L, Lin T, Kietzke T, Chen Z-K (2007) Conjugated copolymers based on fluorene-thieno[3,2-b]thiophene for light-emitting diodes and photovoltaic cells. Macromolecules 40:6164–6171. doi:10.1021/ma070575h
39. Xiao K, Liu Y, Qi T, Zhang W, Wang F, Gao J, Qiu W, Ma Y, Cui G, Chen S, Zhan X, Yu G, Qin J, Hu W, Zhu D (2005) A highly π-stacked organic semiconductor for field-effect transistors based on linearly condensed pentathienoacene. J Am Chem Soc 127:13281–13286. doi:10.1021/ja052816b
40. He M, Li J, Sorensen ML, Zhang F, Hancock RR, Fong HH, Pozdin VA, Smilgies D-M, Malliaras GG (2009) Alkylsubstituted thienothiophene semiconducting materials: structure–property relationships. J Am Chem Soc 131:11930–11938. doi:10.1021/ja903895s
41. Zhang S, He C, Liu Y, Zhan X, Chen J (2009) Synthesis of a soluble conjugated copolymer based on dialkyl-substituted dithienothiophene and its application in photovoltaic cells. Polymer 50:3595–3599
42. Li J, Tan H-S, Chen Z-K, Goh W-P, Wong H-K, Ong K-H, Liu W, Li CM, Ong BS (2011) Dialkyl-substituted dithienothiophene copolymers as polymer semiconductors for thin-film transistors and bulk heterojunction solar cells. Macromolecules 44:690–693. doi:10.1021/ma102247x
43. Takihana Y, Shiotsuki M, Sanda F, Masuda T (2004) Synthesis and properties of carbazole-containing poly(aryleneethynylenes) and poly(aryleneimines). Macromolecules 37:7578–7583. doi:10.1021/ma049391i
44. Leclerc N, Michaud A, Sirois K, Morin JF, Leclerc M (2006) Synthesis of 2,7-carbazolenevinylene-based copolymers and characterization of their photovoltaic properties. Adv Funct Mater 16:1694–1704. doi:10.1002/adfm.200600171
45. Zhang R, Li B, Iovu MC, Jeffries-El M, Sauvé G, Cooper J, Jia S, Tristram-Nagle S, Smilgies DM, Lambeth DN, McCullough RD, Kowalewski T (2006) Nanostructure dependence of field-effect mobility in regioregular poly(3-hexylthiophene) thin film field effect transistors. J Am Chem Soc 128:3480–3481. doi:10.1021/ja055192i
46. Chan S-H, Chen C-P, Chao T-C, Ting C, Lin C-S, Ko B-T (2008) Synthesis, characterization, and photovoltaic properties of novel semiconducting polymers with thiophene–phenylene–thiophene (TPT) as coplanar units. Macromolecules 41:5519–5526. doi:10.1021/ma800494k
47. Anthony JE (2006) Functionalized acenes and heteroacenes for organic electronics. Chem Rev 106:5028–5048. doi:10.1021/cr050966z
48. Okamoto T, Bao Z (2007) Synthesis of solution-soluble pentacene-containing conjugated copolymers. J Am Chem Soc 129:10308–10309. doi:10.1021/ja0725403
49. Okamoto T, Jiang Y, Qu F, Mayer AC, Parmer JE, McGehee MD, Bao Z (2008) Synthesis and characterization of pentacene- and anthradithiophene-fluorene conjugated copolymers synthesized by Suzuki reactions. Macromolecules 41:6977–6980. doi:10.1021/ma800931a
50. Shen P, Sang G, Lu J, Zhao B, Wan M, Zou Y, Li Y, Tan S (2008) Effect of 3D π–π stacking on photovoltaic and electroluminescent properties in triphenylamine-containing poly(*p*-phenylene-vinylene) derivatives. Macromolecules 41:5716–5722. doi:10.1021/ma800847f
51. Murphy AR, Fréchet JMJ (2007) Organic semiconducting oligomers for use in thin film transistors. Chem Rev 107:1066–1096. doi:10.1021/cr0501386
52. Shirota Y, Kageyama H (2007) Charge carrier transporting molecular materials and their applications in devices. Chem Rev 107:953–1010. doi:10.1021/cr050143+
53. Liang Y, Wu Y, Feng D, Tsai S-T, Son H-J, Li G, Yu L (2008) Development of new semiconducting polymers for high performance solar cells. J Am Chem Soc 131:56–57. doi:10.1021/ja808373p
54. Neef CJ, Brotherston ID, Ferraris JP (1999) Synthesis and electronic properties of poly(2-phenylthieno[3,4-b]thiophene): a new low band gap polymer. Chem Mater 11:1957–1958. doi:10.1021/cm9901109
55. Chen H-Y, Hou J, Zhang S, Liang Y, Yang G, Yang Y, Yu L, Wu Y, Li G (2009) Polymer solar cells with enhanced open-circuit voltage and efficiency. Nat Photon 3:649–653
56. Shi C, Yao Y, Yang Y, Pei Q (2006) Regioregular copolymers of 3-alkoxythiophene and their photovoltaic application. J Am Chem Soc 128:8980–8986. doi:10.1021/ja061664x
57. Chen J, Cao Y (2009) Development of novel conjugated donor polymers for high-efficiency bulk-heterojunction photovoltaic devices. Acc Chem Res 42:1709–1718. doi:10.1021/ar900061z

58. Huang C, Lu F, Li Y, Gan H, Jiu T, Xiao J, Xu X, Cui S, Liu H, Zhu D (2007) A novel building block for donor–acceptor conjugated polymers containing perylene, poly(*p*-phenylenevinylene), and fullerene. J Nanosci Nanotechnol 7:1472–1478. doi:10.1166/jnn.2007.329
59. Li G, Shrotriya V, Huang J, Yao Y, Moriarty T, Emery K, Yang Y (2005) High-efficiency solution processable polymer photovoltaic cells by self-organization of polymer blends. Nat Mater 4:864–868
60. Osaka I, McCullough RD (2008) Advances in molecular design and synthesis of regioregular polythiophenes. Acc Chem Res 41:1202–1214. doi:10.1021/ar800130s
61. Chang YT, Hsu SL, Su MH, Wei KH (2007) Soluble phenanthrenyl-imidazole-presenting regioregular poly(3-octylthiophene) copolymers having tunable bandgaps for solar cell applications. Adv Funct Mater 17:3326–3331. doi:10.1002/adfm.200700423
62. Chang Y-T, Hsu S-L, Chen G-Y, Su M-H, Singh TA, Diau EW-G, Wei K-H (2008) Intramolecular donor–acceptor regioregular poly(3-hexylthiophene)s presenting octylphenanthrenyl-imidazole moieties exhibit enhanced charge transfer for heterojunction solar cell applications. Adv Funct Mater 18:2356–2365. doi:10.1002/adfm.200701150
63. Mühlbacher D, Scharber M, Morana M, Zhu Z, Waller D, Gaudiana R, Brabec C (2006) High photovoltaic performance of a low-bandgap polymer. Adv Mater 18:2884–2889. doi:10.1002/adma.200600160
64. Peet J, Kim JY, Coates NE, Ma WL, Moses D, Heeger AJ, Bazan GC (2007) Efficiency enhancement in low-bandgap polymer solar cells by processing with alkane dithiols. Nat Mater 6:497–500
65. Peet J, Soci C, Coffin RC, Nguyen TQ, Mikhailovsky A, Moses D, Bazan GC (2006) Method for increasing the photoconductive response in conjugated polymer/fullerene composites. Appl Phys Lett 89:252105. doi:10.1063/1.2408661
66. Wang EG, Wang L, Lan LF, Luo C, Zhuang WL, Peng JB, Cao Y (2008) High-performance polymer heterojunction solar cells of a polysilafluorene derivative. Appl Phys Lett 92:033307. doi:10.1063/1.2836266
67. Hou J, Chen H-Y, Zhang S, Li G, Yang Y (2008) Synthesis, characterization, and photovoltaic properties of a low band gap polymer based on silole-containing polythiophenes and 2,1,3-benzothiadiazole. J Am Chem Soc 130:16144–16145. doi:10.1021/ja806687u
68. Coffin RC, Peet J, Rogers J, Bazan GC (2009) Streamlined microwave-assisted preparation of narrow-bandgap conjugated polymers for high-performance bulk heterojunction solar cells. Nat Chem 1:657–661
69. Chen H-Y, Hou J, Hayden AE, Yang H, Houk KN, Yang Y (2010) Silicon atom substitution enhances interchain packing in a thiophene-based polymer system. Adv Mater 22:371–375. doi:10.1002/adma.200902469
70. Amb CM, Chen S, Graham KR, Subbiah J, Small CE, So F, Reynolds JR (2011) Dithienogermole as a fused electron donor in bulk heterojunction solar cells. J Am Chem Soc 133:10062–10065. doi:10.1021/ja204056m
71. Chu T-Y, Lu J, Beaupré S, Zhang Y, Pouliot J-RM, Wakim S, Zhou J, Leclerc M, Li Z, Ding J, Tao Y (2011) Bulk heterojunction solar cells using thieno[3,4-c]pyrrole-4,6-dione and dithieno[3,2-b:2′,3′-d]silole copolymer with a power conversion efficiency of 7.3%. J Am Chem Soc 133:4250–4253
72. Wang M, Hu X, Liu P, Li W, Gong X, Huang F, Cao Y (2011) Donor–acceptor conjugated polymer based on naphtho[1,2-c:5,6-c]bis[1,2,5]thiadiazole for high-performance polymer solar cells. J Am Chem Soc 133:9638–9641. doi:10.1021/ja201131h
73. Scharber MC, Mühlbacher D, Koppe M, Denk P, Waldauf C, Heeger AJ, Brabec CJ (2006) Design rules for donors in bulk-heterojunction solar cells—towards 10 % energy-conversion efficiency. Adv Mater 18:789–794. doi:10.1002/adma.200501717
74. Walker B, Tamayo AB, Dang X-D, Zalar P, Seo JH, Garcia A, Tantiwiwat M, Nguyen T-Q (2009) nanoscale phase separation and high photovoltaic efficiency in solution-processed, small-molecule bulk heterojunction solar cells. Adv Funct Mater 19:3063–3069. doi:10.1002/adfm.200900832
75. Tamayo AB, Xuan-Dang D, Walker B, Junghwa S, Kent T, Thuc-Quyen N (2009) A low band gap, solution processable oligothiophene with a dialkylated diketopyrrolopyrrole chromophore for use in bulk heterojunction solar cells. Appl Phys Lett 94:103301–103303. doi:10.1063/1.3086897
76. Loser S, Bruns CJ, Miyauchi H, RoP Ortiz, Facchetti A, Stupp SI, Marks TJ (2011) A naphthodithiophene-diketopyrrolopyrrole donor molecule for efficient solution-processed solar cells. J Am Chem Soc 133:8142–8145. doi:10.1021/ja202791n

77. Ha JS, Kim KH, Choi DH (2011) 2,5-bis(2-octyldodecyl)pyrrolo[3,4-c]pyrrole-1, 4-(2H,5H)-dione-based donor–acceptor alternating copolymer bearing 5,5′-di(thiophen-2-yl)-2,2′-biselenophene exhibiting 1.5 $cm^2 V^{-1} s^{-1}$ hole mobility in thin-film transistors. J Am Chem Soc 133:10364–10367. doi:10.1021/ja203189h
78. Bijleveld JC, Zoombelt AP, Mathijssen SGJ, Wienk MM, Turbiez M, de Leeuw DM, Janssen RAJ (2009) Poly(diketopyrrolopyrrole-terthiophene) for ambipolar logic and photovoltaics. J Am Chem Soc 131:16616–16617. doi:10.1021/ja907506r
79. Bijleveld JC, Gevaerts VS, Nuzzo D Di, Turbiez M, Mathijssen SGJ, de Leeuw DM, Wienk MM, Janssen RAJ (2010) Efficient solar cells based on an easily accessible diketopyrrolopyrrole polymer. Adv Mater 22:E242–E246. doi:10.1002/adma.201001449
80. Woo CH, Beaujuge PM, Holcombe TW, Lee OP, Fréchet JMJ (2010) Incorporation of furan into low band-gap polymers for efficient solar cells. J Am Chem Soc 132:15547–15549. doi:10.1021/ja108115y
81. Wienk MM, Turbiez M, Gilot J, Janssen RAJ (2008) Narrow-bandgap diketo-pyrrolo-pyrrole polymer solar cells: the effect of processing on the performance. Adv Mater 20:2556–2560. doi:10.1002/adma.200800456
82. Zoombelt AP, Mathijssen SGJ, Turbiez MGR, Wienk MM, Janssen RAJ (2010) Small band gap polymers based on diketopyrrolopyrrole. J Mater Chem 20:2240–2246
83. Xiao S, Stuart AC, Liu S, Zhou H, You W (2010) Conjugated polymer based on polycyclic aromatics for bulk heterojunction organic solar cells: a case study of quadrathienonaphthalene polymers with 2% efficiency. Adv Funct Mater 20:635–643. doi:10.1002/adfm.200901407
84. Zhou H, Yang L, Stuart AC, Price SC, Liu S, You W (2011) Development of fluorinated benzothiadiazole as a structural unit for a polymer solar cell of 7 % efficiency. Angew Chem Int Ed 50:2995–2998. doi:10.1002/anie.201005451
85. Price SC, Stuart AC, Yang L, Zhou H, You W (2011) Fluorine substituted conjugated polymer of medium band gap yields 7% efficiency in polymer–fullerene solar cells. J Am Chem Soc 133:4625–4631. doi:10.1021/ja1112595
86. Blouin N, Michaud A, Gendron D, Wakim S, Blair E, Neagu-Plesu R, Belletête M, Durocher G, Tao Y, Leclerc M (2007) Toward a rational design of poly(2,7-carbazole) derivatives for solar cells. J Am Chem Soc 130:732–742. doi:10.1021/ja0771989
87. Seo JH, Gutacker A, Sun Y, Wu H, Huang F, Cao Y, Scherf U, Heeger AJ, Bazan GC (2011) Improved high-efficiency organic solar cells via incorporation of a conjugated polyelectrolyte interlayer. J Am Chem Soc 133:8416–8419. doi:10.1021/ja2037673
88. Li Y, Wu Y, Ong BS (2006) Polyindolo[3,2-b]carbazoles: a new class of p-channel semiconductor polymers for organic thin-film transistors. Macromolecules 39:6521–6527. doi:10.1021/ma0612069
89. Wu YL, Li YN, Gardner S, Ong BS (2005) Indolo 3,2-b carbazole-based thin-film transistors with high mobility and stability. J Am Chem Soc 127:614–618. doi:10.1021/ja0456149
90. Tsai J-H, Chueh C–C, Lai M-H, Wang C-F, Chen W-C, Ko B-T, Ting C (2009) Synthesis of new indolocarbazole-acceptor alternating conjugated copolymers and their applications to thin film transistors and photovoltaic cells. Macromolecules 42:1897–1905. doi:10.1021/ma802720n
91. Li Y, Xu B, Li H, Cheng W, Xue L, Chen F, Lu H, Tian W (2011) Molecular engineering of copolymers with donor–acceptor structure for bulk heterojunction photovoltaic cells toward high photovoltaic performance. J Phys Chem C 115:2386–2397. doi:10.1021/jp1090872
92. Cravino A, Sariciftci NS (2003) Organic electronics: molecules as bipolar conductors. Nat Mater 2:360–361
93. Xu JH, Li YL, Guo ZX, Li FY, Shi ZQ, Pan CY, Zhu DB (2000) A novel reaction: 60,70 fullerene reacting with 4,4,5,5-tetramethylimidazoline-2-thione and alpha-aminoacids as carbene reaction. J Phys Chem Solids 61:1081–1088. doi:10.1016/s0022-3697(99)00365-0
94. Shi ZQ, Li YL, Xu JH, Ge ZX, Zhu DB (2000) Covalently linked 60,70 fullerenes-nitroxide unit for synthesis and characterization. J Phys Chem Solids 61:1095–1099. doi:10.1016/s0022-3697(99)00367-4
95. Ge ZX, Li YL, Shi ZQ, Bai FF, Zhu DB (2000) Synthesis and photophysical characterization of a new crown ether-bearing 70 fulleropyrrolidine derivative. J Phys Chem Solids 61:1075–1079. doi:10.1016/s0022-3697(99)00364-9
96. Du CM, Li YL, Wang S, Shi ZQ, Xiao SX, Zhu DB (2001) Synthesis and characterization of 60 fullerene-substituted oligopyridines ruthenium complexes. Synth Met 124:287–289. doi:10.1016/s0379-6779(01)00363-0

97. Xiao SQ, Li YL, Fang HJ, Li HM, Liu HB, Shi ZQ, Jiang L, Zhu DB (2002) Synthesis and characterization of three novel 60 fullerene derivatives toward self-assembled nanoparticles through interaction of hydrogen bonding. Org Lett 4:3063–3066. doi:10.1021/ol026386v
98. Li YL, Wang S, Li FY, Du CM, Shi ZQ, Zhu DB, Song YL (2001) Preparation and optical limiting properties of polycarbonates containing fullerene unit. Chem Phys Lett 337:403–407. doi:10.1016/s0009-2614(01)00211-1
99. Liu C, Li Y, Li C, Li W, Zhou C, Liu H, Bo Z, Li Y (2009) New methanofullerenes containing amide as electron acceptor for construction photovoltaic devices. J Phys Chem C 113:21970–21975. doi:10.1021/jp907240n
100. Li YJ, Liu Y, Wang N, Li YL, Liu HB, Lu FS, Zhuang JP, Zhu DB (2005) Self-assembled monolayers of C-60-perylenetetracarboxylic diimide-C-60 triad on indium tin oxide surface. Carbon 43:1968–1975. doi:10.1016/j.carbon.2005.03.005
101. Li YJ, Li YL, Liu HB, Wang S, Wang N, Zhuang JP, Li XF, He XR, Zhu DB (2005) Self-assembled monolayers of porphyrin-perylenetetracarboxylic diimide-60 fullerene on indium tin oxide electrodes: enhancement of light harvesting in the visible light region. Nanotechnology 16:1899–1904. doi:10.1088/0957-4484/16/9/080
102. Li Y, Li Y, Li J, Li C, Liu X, Yuan M, Liu H, Wang S (2006) Synthesis, characterization, and self-assembly of nitrogen-containing heterocoronenetetracarboxylic acid diimide analogues: Photocyclization of N-heterocycle-substituted perylene bisimides. Chem Eur J 12:8378–8385. doi:10.1002/chem.200600605
103. Li Y, Zheng H, Li Y, Wang S, Wu Z, Liu P, Gao Z, Liu H (2007) Photonic logic gates based on control of FRET by a solvatochromic perylene bisimide. J Org Chem 72:2878–2885. doi:10.1021/jo0624748
104. He X, Liu H, Wang N, Ai X, Wang S, Li Y, Huang C, Cui S, Li Y, Zhu D (2005) Synthesis and characterization of new types of perylene bisimide-containing conjugated copolymers. Macromol Rapid Commun 26:721–727. doi:10.1002/marc.200400660
105. Li Y, Gan Z, Wang N, He X, Li Y, Wang S, Liu H, Araki Y, Ito O, Zhu D (2006) Synthesis and characterization of porphyrin–ferrocene–fullerene triads. Tetrahedron 62:4285–4293. doi:10.1016/j.tet.2006.02.076
106. Xiao SQ, Li YL, Li YJ, Zhuang JP, Wang N, Liu HB, Ning B, Liu Y, Lu FS, Fan LZ, Yang CH, Li YF, Zhu DB (2004) 60 Fullerene-based molecular triads with expanded absorptions in the visible region: Synthesis and photovoltaic properties. J Phys Chem B 108:16677–16685. doi:10.1021/jp0478413
107. Xiao SQ, El-Khouly ME, Li YL, Gan ZH, Liu HB, Jiang L, Araki Y, Ito O, Zhu D (2005) Dyads and triads containing perylenetetracarboxylic diimide and porphyrin: efficient photoinduced electron transfer elicited via both excited singlet states. J Phys Chem B 109:3658–3667. doi:10.1021/jp045163e
108. Ramos AM, Rispens MT, van Duren JKJ, Hummelen JC, Janssen RAJ (2001) Photoinduced electron transfer and photovoltaic devices of a conjugated polymer with pendant fullerenes. J Am Chem Soc 123:6714–6715. doi:10.1021/ja015614y
109. Gomez R, Veldman D, Blanco R, Seoane C, Segura JL, Janssen RAJ (2007) Energy and electron transfer in a poly(fluorene-alt-phenylene) bearing perylenediimides as pendant electron acceptor groups. Macromolecules 40:2760–2772. doi:10.1021/ma070026b
110. Hains AW, Liang Z, Woodhouse MA, Gregg BA (2010) Molecular semiconductors in organic photovoltaic cells. Chem Rev 110:6689–6735. doi:10.1021/cr9002984
111. Kaunisto K, Chukharev V, Tkachenko NV, Efimov A, Lemmetyinen H (2009) Energy and electron transfer in multilayer films containing porphyrin–fullerene dyad. J Phy Chem C 113:3819–3825. doi:10.1021/jp807962j
112. Liddell PA, Kodis G, Moore AL, Moore TA, Gust D (2002) Photonic switching of photoinduced electron transfer in a dithienylethene–porphyrin–fullerene triad molecule. J Am Chem Soc 124:7668–7669. doi:10.1021/ja026327c
113. Huang C, Wen L, Liu H, Li Y, Liu X, Yuan M, Zhai J, Jiang L, Zhu D (2009) Controllable growth of 0D to multidimensional nanostructures of a novel porphyrin molecule. Adv Mater 21:1721–1725. doi:10.1002/adma.200802114
114. Li Y, Li X, Li Y, Liu H, Wang S, Gan H, Li J, Wang N, He X, Zhu D (2006) Controlled self-assembly behavior of an amphiphilic bisporphyrin–bipyridinium–palladium complex: from multibilayer vesicles to hollow capsules. Angew Chem Int Ed 45:3639–3643. doi:10.1002/anie.200600554
115. Huang C, Li Y, Song Y, Li Y, Liu H, Zhu D (2010) Ordered nanosphere alignment of porphyrin for the improvement of nonlinear optical properties. Adv Mater 22:3532–3536. doi:10.1002/adma.200904421

116. Jiu T, Li Y, Gan H, Li Y, Liu H, Wang S, Zhou W, Wang C, Li X, Liu X, Zhu D (2007) Synthesis of oligo(*p*-phenylene vinylene)-porphyrin-oligo(*p*-phenylene vinylene) triads as antenna molecules for energy transfer. Tetrahedron 63:232–240. doi:10.1016/j.tet.2006.10.029
117. Huang C, Li Y, Yang Je, Cheng N, Liu H, Li Y (2010) Construction of multidimensional nanostructures by self-assembly of a porphyrin analogue. Chem Commun 46:3161–3163. doi:10.1039/b927059k
118. Lu F, Xiao S, Li Y, Liu H, Li H, Zhuang J, Liu Y, Wang N, He X, Li X, Gan L, Zhu D (2004) Synthesis and chemical properties of conjugated polyacetylenes having pendant fullerene and/or porphyrin units. Macromolecules 37:7444–7450. doi:10.1021/ma0490045
119. Wang N, Li Y, Lu F, Liu Y, He X, Jiang L, Zhuang J, Li X, Li Y, Wang S, Liu H, Zhu D (2005) Fabrication of novel conjugated polymer nanostructure: porphyrins and fullerenes conjugately linked to the polyacetylene backbone as pendant groups. J Polym Sci A 43:2851–2861. doi:10.1002/pola.20757
120. Liu Y, Wang N, Li Y, Liu H, Li Y, Xiao J, Xu X, Huang C, Cui S, Zhu D (2005) A new class of conjugated polyacetylenes having perylene bisimide units and pendant fullerene or porphyrin groups. Macromolecules 38:4880–4887. doi:10.1021/ma050434k
121. Huang C, Wang N, Li Y, Li C, Li J, Liu H, Zhu D (2006) A new class of conjugated polymers having porphyrin, poly(*p*-phenylenevinylene), and fullerene units for efficient electron transfer. Macromolecules 39:5319–5325. doi:10.1021/ma060084h
122. Tan Z, Hou JH, He YJ, Zhou EJ, Yang CH, Li YF (2007) Synthesis and photovoltaic properties of a donor-acceptor double-cable polythiophene with high content of C-60 pendant. Macromolecules 40:1868–1873. doi:10.1021/ma070052+
123. Schulz GL, Holdcroft S (2008) Conjugated polymers bearing iridium complexes for triplet photovoltaic devices. Chem Mater 20:5351–5355. doi:10.1021/cm800955f
124. Shao Y, Yang Y (2005) Efficient organic heterojunction photovoltaic cells based on triplet materials. Adv Mater 17:2841–2844. doi:10.1002/adma.200501297
125. Fukuzumi S, Endo Y, Imahori H (2002) A negative temperature dependence of the electron self-exchange rates of zinc porphyrin π-radical cations. J Am Chem Soc 124:10974–10975. doi:10.1021/ja026089l
126. Sun Q, Dai L, Zhou X, Li L, Li Q (2007) Bilayer- and bulk-heterojunction solar cells using liquid crystalline porphyrins as donors by solution processing. Appl Phys Lett 91:253505. doi:10.1063/1.2823586
127. Zhan H, Lamare S, Ng A, Kenny T, Guernon H, Chan W-K, Djurišić AB, Harvey PD, Wong W-Y (2011) Synthesis and photovoltaic properties of new metalloporphyrin-containing polyplatinyne polymers. Macromolecules 44:5155–5167. doi:10.1021/ma2006206
128. Wu P-T, Bull T, Kim FS, Luscombe CK, Jenekhe SA (2009) Organometallic donor–acceptor conjugated polymer semiconductors: tunable optical, electrochemical, charge transport, and photovoltaic properties. Macromolecules 42:671–681. doi:10.1021/ma8016508
129. Silverman EE, Cardolaccia T, Zhao X, Kim K-Y, Haskins-Glusac K, Schanze KS (2005) The triplet state in Pt-acetylide oligomers, polymers and copolymers. Coord Chem Rev 249:1491–1500
130. Clem TA, Kavulak DFJ, Westling EJ, Fréchet JMJ (2009) Cyclometalated platinum polymers: synthesis, photophysical properties, and photovoltaic performance. Chem Mater 22:1977–1987. doi:10.1021/cm9029038
131. Greenham NC, Moratti SC, Bradley DDC, Friend RH, Holmes AB (1993) Efficient light-emitting-diodes based on polymers with high electron-affinities. Nature 365:628–630. doi:10.1038/365628a0
132. Knupfer M (2003) Exciton binding energies in organic semiconductors. Appl Phys A 77:623–626. doi:10.1007/s00339-003-2182-9
133. Coropceanu V, Cornil J, da Silva Filho DA, Olivier Y, Silbey R, Bredas J-L (2007) Charge transport in organic semiconductors. Chem Rev 107:926–952. doi:10.1021/cr050140x
134. Darling SB (2008) Isolating the effect of torsional defects on mobility and band gap in conjugated polymers. J Phys Chem B 112:8891–8895. doi:10.1021/jp8017919
135. Darling SB, Sternberg M (2009) Importance of side chains and backbone length in defect modeling of poly(3-alkylthiophenes). J Phys Chem B 113:6215–6218. doi:10.1021/jp808045j
136. Liu H, Zhao Q, Li Y, Liu Y, Lu F, Zhuang J, Wang S, Jiang L, Zhu D, Yu D, Chi L (2005) Field emission properties of large-area nanowires of organic charge-transfer complexes. J Am Chem Soc 127:1120–1121. doi:10.1021/ja0438359
137. Cui S, Li YL, Guo YB, Liu HBA, Song YL, Xu JL, Lv J, Zhu M, Zhu DB (2008) Fabrication and field-emission properties of large-area nanostructures of the organic charge-transfer complex Cu-TCNAQ. Adv Mater 20:309. doi:10.1002/adma.200701617

138. Liu H, Li Y, Jiang L, Luo H, Xiao S, Fang H, Li H, Zhu D, Yu D, Xu J, Xiang B (2002) Imaging as-grown [60]fullerene nanotubes by template technique. J Am Chem Soc 124:13370–13371. doi:10.1021/ja0280527
139. Guo Y, Tang Q, Liu H, Zhang Y, Li Y, Hu W, Wang S, Zhu D (2008) Light-controlled organic/inorganic P–N junction nanowires. J Am Chem Soc 130:9198–9199. doi:10.1021/ja8021494
140. Guo Y, Li Y, Li Y, Liu H, Li G, Zhao Y, Lin H (2011) Construction of heterojunction nanowires from polythiophene/polypyrrole for applications as efficient switches. Chem Asian J 6:98–102. doi:10.1002/asia.201000400
141. Zuo Z, Guo Y, Li Y, Lv J, Liu H, Xu J, Li Y (2009) Construction of large-scale highly ordered macroporous monoliths of pi-conjugated polymers. Macromol Rapid Commun 30:1940–1944. doi:10.1002/marc.200900411
142. Gan H, Liu H, Li Y, Zhao Q, Li Y, Wang S, Jiu T, Wang N, He X, Yu D, Zhu D (2005) Fabrication of polydiacetylene nanowires by associated self-polymerization and self-assembly processes for efficient field emission properties. J Am Chem Soc 127:12452–12453. doi:10.1021/ja053352k
143. Guo Y, Zhang Y, Liu H, Lai S-W, Li Y, Li Y, Hu W, Wang S, Che C-M, Zhu D (2010) Assembled organic/inorganic p–n junction interface and photovoltaic cell on a single nanowire. J Phys Chem L 1:327–330. doi:10.1021/jz9002058
144. Yang X, van Duren JKJ, Janssen RAJ, Michels MAJ, Loos J (2004) Morphology and thermal stability of the active layer in poly(*p*-phenylenevinylene)/methanofullerene plastic photovoltaic devices. Macromolecules 37:2151–2158. doi:10.1021/ma035620+
145. Shikler R, Chiesa M, Friend RH (2006) Photovoltaic performance and morphology of polyfluorene blends: the influence of phase separation evolution. Macromolecules 39:5393–5399. doi:10.1021/ma060421m
146. McNeill CR, Westenhoff S, Groves C, Friend RH, Greenham NC (2007) Influence of nanoscale phase separation on the charge generation dynamics and photovoltaic performance of conjugated polymer blends: balancing charge generation and separation. J Phys Chem C 111:19153–19160. doi:10.1021/jp075904m
147. Thomas EL, Lescanec RL (1994) Phase morphology in block-copolymer systems. Phil Trans R Soc Lond Ser A 348:149–166
148. Lee M, Cho B-K, Zin W-C (2001) Supramolecular structures from rod–coil block copolymers. Chem Rev 101:3869–3892. doi:10.1021/cr0001131
149. Segalman RA, McCulloch B, Kirmayer S, Urban JJ (2009) Block copolymers for organic optoelectronics. Macromolecules 42:9205–9216. doi:10.1021/ma901350w
150. Botiz I, Darling SB (2009) Self-assembly of poly(3-hexylthiophene)-*block*-polylactide block copolymer and subsequent incorporation of electron acceptor material. Macromolecules 42:8211–8217. doi:10.1021/ma901420h
151. Sirringhaus H, Tessler N, Friend RH (1998) Integrated optoelectronic devices based on conjugated polymers. Science 280:1741–1744. doi:10.1126/science.280.5370.1741
152. Shrotriya V, Ouyang J, Tseng RJ, Li G, Yang Y (2005) Absorption spectra modification in poly(3-hexylthiophene):methanofullerene blend thin films. Chem Phys Lett 411:138–143
153. Boudouris BW, Frisbie CD, Hillmyer MA (2007) Nanoporous poly(3-alkylthiophene) thin films generated from block copolymer templates. Macromolecules 41:67–75. doi:10.1021/ma071626d
154. Ren G, Wu P-T, Jenekhe SA (2010) Solar cells based on block copolymer semiconductor nanowires: effects of nanowire aspect ratio. ACS Nano 5:376–384. doi:10.1021/nn1017632
155. Tao Y, McCulloch B, Kim S, Segalman RA (2009) The relationship between morphology and performance of donor–acceptor rod-coil block copolymer solar cells. Soft Matter 5:4219–4230
156. Zhang Q, Cirpan A, Russell TP, Emrick T (2009) Donor–acceptor poly(thiophene-block-perylene diimide) copolymers: synthesis and solar cell fabrication. Macromolecules 42:1079–1082. doi:10.1021/ma801504e
157. Dante M, Yang C, Walker B, Wudl F, Nguyen T-Q (2010) Self-assembly and charge-transport properties of a polythiophene–fullerene triblock copolymer. Adv Mater 22:1835–1839. doi:10.1002/adma.200902696
158. Stalmach U, de Boer B, Videlot C, van Hutten PF, Hadziioannou G (2000) Semiconducting diblock copolymers synthesized by means of controlled radical polymerization techniques. J Am Chem Soc 122:5464–5472. doi:10.1021/ja000160a
159. Barrau S, Heiser T, Richard F, Brochon C, Ngov C, van de Wetering K, Hadziioannou G, Anokhin DV, Ivanov DA (2008) Self-assembling of novel fullerene-grafted donor–acceptor rod–coil block copolymers. Macromolecules 41:2701–2710. doi:10.1021/ma7022099